PNAS
www.pnas.org

Supplementary Information for

Native American Fire Management at an Ancient Wildland-Urban Interface in the Southwest US

Christopher I. Roos, Thomas W. Swetnam, Matthew J. Liebmann, Rachel A. Loehman, T. J. Ferguson, John R. Welch, Ellis Q. Margolis, Christopher H. Guiterman, William C. Hockaday, Michael Aiuvalasit, Jenna Battillo, Josh Farella, and Christopher A. Kiahtipes

Christopher Roos
Email: croos@smu.edu

This PDF file includes:

Geoarchaeological field and lab methods

Sections of soil and sediment stratigraphy were observed by manually trenching alluvial channel fan terraces (Monument Canyon 4), cleaning natural exposures (Monument Canyon 4B), or coring terrestrial (Banco Bonito 1 and 2; Cebollita Springs 3; San Juan 2) and bog contexts (Lake Fork Canyon 3B and 3C). Manual trenches were roughly 1 m wide and excavated until coarse channel lag or bedrock prohibited further excavation. Profiles were cleaned and sprayed with water until uniformly moist to measure and describe sedimentary strata and soil horizons using standard terminology (1). Undisturbed monoliths were carved from the center of the profile for later micromorphological analysis of soil thin sections (2, 3), although micromorphology is not presented here. We collected a continuous column of bulk samples at 2cm intervals along the margin of the monoliths. This continuous column of bulk samples was used for measuring gravel %, grain-size (aggregated in 4-10cm thick intervals by horizon), pH (intermittently, every 10cm by horizon), charcoal and organic matter. We collected 4-10 cm thick samples (by horizon) for palynology along the other margin of the monolith.

From terrestrial contexts, we extracted 3 cm diameter cores in 90cm intervals using an electric percussion hammer until the corer refused (typically on bedrock or cobble channel lag). We extracted four cores from each location, each within ~30-50 cm of each other as the corners of a square. One core was opened in the field for stratigraphic descriptions and sampled at 5 cm continuous intervals for pH, gravel %, grain-size (at 5 cm or aggregated at 10cm intervals in the lab), charcoal and organic matter. The three other replicate cores were (1) used for pollen (at 10cm intervals to accommodate poor preservation and rapid sedimentation), (2) for extracting charcoal for radiocarbon dating (at 5 cm intervals), and (3) preserved for embedding in polyester resin for soil micromorphology (at 35cm intervals), which is not presented here. Pedogenic mixing generated intersample autocorrelation that made sample resolution finer than 5 cm continuous intervals unnecessarily redundant.

At the bog in Lake Fork Canyon, a 5 cm diameter piston core was used to extract wetland sediments down to ~1-1.5 m. Extracted bog cores were wrapped in plastic for transport back to Southern Methodist University (SMU) where they were subdivided in 1 cm (LFC 3C) or 2 cm increments (LFC 3B) for measuring charcoal and organic matter. For all extracted terrestrial and palustrine cores, samples were regularly compacted up to 15% in the process of coring. Reported depths for all cores (terrestrial and palustrine) are based on the extracted cores, not the downhole measurements, which were not possible at all coring locations. Maximum downhole depth was 6.4 m but maximum extracted core depth (at Banco Bonito 2) was 5.6 m.

Gravel weight percentages were calculated by dry sieving the >2 mm fraction from bulk samples. The <2 mm fraction was retained for other analyses. At SMU, we measured pH with an Eco Tester pH 2 meter on a 1:1 soil:deionized water slurry of 1 g powdered sub-samples < 2mm. Measurement was calibrated with buffers at pH 4, pH 7, and pH 10. Grain size (percentages of sand [63 – 2000 μm], silt [4 – 63 μm], and clay [<4 μm]) were measured by weight percent after removing carbonates with 0.5 N HCl, digesting organic matter with 30% H_2O_2, deflocculating with 5% sodium hexametaphosphate, and wet sieved at 63 μm to separate sands from silt and clay (4). Silt and clay fractions were estimated using Stoke's law and the pipette method (4). Organic matter and charcoal were measured using a stepped 80% HNO_3 digestion and loss-on-ignition method (5). Organic matter was estimated from the weight loss during HNO_3 digestion. We estimated charcoal by the weight loss on ignition after HNO_3 treatment. Macroscopic charcoal (>125 μm) concentrations were also quantified for Lake Fork Canyon bog cores following Whitlock and Anderson (6) and Rhodes (7)

Individual or aggregated charcoal fragments were pre-treated for radiocarbon measurement using a standard Acid-Base-Acid (ABA) pretreatment of sequential 3N HCl-NaOH-3N HCl (8). Bulk soil or sediment samples were either treated by 80% HNO3 or ABA of the <250 μm fraction. With few exceptions, pretreated samples were measured for radiocarbon content at the University of California–Irvine Keck Carbon Cycle Accelerator Mass Spectrometry lab. Where appropriate, radiocarbon age estimates were calibrated using IntCal13 (9) using stratigraphic and tree-ring evidence in the Bayesian program, BCal (10). Age-depth models were calculated using the CLAM program in R (11). Radiocarbon ages that were too old for the age-depth model were removed and considered evidence of enhanced upland erosion that displaced and redeposited older charcoal in the sedimentary locality.

For pollen analysis, we subsampled 3 ml of each sample, added a *Lycopodium* sp. tablet spike to derive pollen concentrations (2 tablets, batch #414831) (12, 13), and sieved them at 150 µm after treatment with HCl. Pollen was extracted using established methods (14, 15), which include treatments with HCl to remove carbonates, HF to remove silicates, KOH to remove complex organic molecules, and acetolysis to remove cellulose and lignin. A zinc bromide solution with a specific gravity of 2.0 was used to segregate the remaining minerals and the organic sample fraction, which was pipetted off in ethanol. Pollen samples were stored in sealed vials with glycerin and mounted in glycerin on glass slides for analysis.

Slides were analyzed using binocular light microscopes at 400 x magnification. Samples were analyzed until a minimum of 200 pollen identifications were made or 300 *Lycopodium* tracer spores were encountered. The coprophilic fungi *Sporormiella* was also tallied but was not included in the pollen counts. We identified fossil pollen using reference texts (16, 17), modern comparative slides, and online comparative image databases such as PalDat Palynological Database (18) and a now-defunct image database formerly maintained by the University of Arizona. Data are plotted using R (19) and will be archived at Neotoma (20).

Biomarker extraction from Banco Bonito 1. Approximately 7 g of freeze-dried and homogenized sediment were mixed with 1 g anhydrous sodium sulfate, a drying agent, and 1 g diatomaceous earth (Fisher scientific), a filtration aid to ensure homogenous solvent flow through the sample. A solvent-washed, stainless steel, extraction cell (33 mL volume) was prepared by inserting a 20mm cellulose filter (2μm pore size, Restek) followed by 1 g silica gel as a solid phase adsorbent (chromatography grade, 100 mesh, Macron Chemical), followed by a second cellulose filter, and the sample mixture. Dead volume in the headspace of the extraction cell was filled with diatomaceous earth prior to attaching the upper cap. Cells were installed in Dionex 200 Accelerated Solvent Extractor, and each sample was extracted three times with a mixture of 90% dichloromethane (DCM) and 10% methanol (HPLC grade, BDH Chemical) at temperature of 100 ^{o}C and pressure of 1,500 psi for 5 minutes per extraction cycle. Lipid extracts were flushed from the sample into 70 mL amber glass vial by compressed N_2 gas (99.999%), and immediately concentrated to a volume of 1 mL under a stream of N_2 gas at 30 ^{o}C.

Biomarker derivatization and GCMS quantification from Banco Bonito 1. Concentrated extracts were transferred to 2mL GC vials and polar lipids were silylated by adding 25 µl bis (trimethylsilyl) trifluoroacetamide (BSTFA) and 25 µL pyridine, capped tightly, and heated to 65°C for 60 mins. Samples were analyzed By GCMS within 12 hours of silylation using an Agilent 6890 GC Plus with Agilent 5973A Quadrupole mass selective (MS) detector and Chemstation software. The GC column was a Restek silica capillary 30m x 0.25mm with RX-5 stationary phase. The GC temperature was ramped from 50-310°C with 5°C/min and held at 310^{o}C for 10 minutes with Helium carrier gas flow rate of 1ml/min and 20 kPa pressure. The ion source and MS were operated in positive ion mode under the following conditions: electron voltage 70eV, source temperature 230°C, quadrupole temperature 150°C multiplier voltage 2000 V, interface temperature 280°C. Trimethyl silylated sterols and were identified by comparison to authentic standards (Sigma Aldrich). Stanols were identified by selected ion search for characteristic ion 215 m/z following Battistel and others (21). Peak assignments were confirmed by > 80% similarity to mass spectra NIST08 and Wiley Geolipid reference library. Comparisons of down-core relative abundance were made on the basis of mass-normalized total ion current obtained from peak integration (mV·s / g).

Stratigraphic paleoecological localities

Banco Bonito 1 (BBO 1). Banco Bonito locality 1 (BBO 1) is a coring location within a >30 m deep, steep-sided explosion pit on the Banco Bonito Rhyolite (Fig. S1). Explosion pits form from the degassing of volatiles as they are concentrated towards the distal end of silicious lava flows, so they are contemporaneous features with the rhyolite flow in which they are found (22). The small hydrological catchment for the core spot (8.5 ha) is almost exclusively within the explosion pit, so hillslope and colluvial sediments are from extremely localized sources. Vegetation within and around the basin is almost entirely ponderosa pine forest (*Pinus ponderosa*) but the north facing slope on the south end of the explosion pit has aspen (*Populus tremuloides*), and mixed

conifer vegetation with Douglas fir (*Pseudotsuga menziesii)*, and rare white fir (*Abies concolor*), and Southwestern white pine (*Pinus strobiformis*). Four 515 cm deep cores were extracted from the center of the basin, with the corer refusing on rhyolite bedrock in each instance (Fig. S2). Stratigraphic descriptions (Table S1), radiocarbon dates (Table S2), and the age-depth model (Fig. S3) can be found below.

The basal sediments (Lithostratigraphic Unit I) represent fine-grained eolian deposition at the bottom of the explosion pit after it formed and the rhyolite cooled (Table S1 and Fig. S4). A bulk radiocarbon date from this unit indicates that it formed roughly 26 ka cal BP. Although this is young relative to the conventional emplacement age for the Banco Bonito Rhyolite of 40±5 ka BP (23, 24), it is consistent with an the youngest ^{21}Ne cosmogenic surface exposure date and optically stimulated luminescence age estimates of roughly 26-27 ka BP (25, 26). Deposition was exclusively eolian for some time, perhaps through the Last Glacial Maximum (26-16 ka BP), building up 15cm of silt loams before the rhyolite had weathered sufficiently for colluvium to become a major contributor to local sedimentation, but this transition is not dated.

At some point in the terminal Pleistocene, rhyolite weathering developed to the extent that sedimentation was dominated by poorly sorted coarse, sandy and pebbly colluvium (Lithostratigraphic Unit II). Within this unit, there is a single buried soil surface (Ab5) with a bulk age dating to the Younger Dryas chronozone (~12-12.5 ka cal BP), although this soil appears to have been stable long enough to generate subsoil weathering and a Bw horizon. The Younger Dryas soil is buried by ongoing coarse, sandy and gravelly colluvium that is capped with an Early Holocene soil (Ab4; ~9.5 ka cal BP dating charcoal fragments) with a much finer texture, perhaps indicative of greater eolian input to hillslope-derived colluvium (Lithostratigraphic Unit III). A radiocarbon age reversal in the colluvium above Ab5 may indicate soil development on the hillslopes prior to reactivation of colluvial erosion/deposition. Prior to the formation of the Ab4 soil, charcoal concentrations were low and varied little. Charcoal in the Unit I eolian deposits are comparable to the rest of Unit II, suggesting that most measurable charcoal through the Last Glacial Maximum into the Early Holocene was non-local and derived from eolian transport. By the formation of the Ab4 horizon, however, charcoal abundances increase and may represent the beginning of local fire activity around the BBO 1 explosion pit by ~9.5 ka cal BP. Charcoal concentrations steadily increase from this point to the surface, where they decline at the very top. From Ab4 upwards in Unit III, deposits indicate nearly contemporaneous deposition of mixed eolian and colluvial sediments with soil formation. The upper ~3m of the cores are represented by more or less welded, buried surfaces within one thick cumulic soil. From 192-312 cm, surfaces are better separated and identifiable as distinct, relatively young soils forming between roughly 4 ka and 9.5 ka cal BP. From 5-192cm, buried soil surfaces are indistinct and welded into an overthickened A horizon, although subhorizons A2 and A3 may have been paleo-surfaces that have been welded into the 2 m thick cumulic soil.

The cumulic modern soil is characterized by increasing charcoal concentrations, with the greatest concentrations achieved in the uppermost A1 horizon, which yielded a radiocarbon age on charred bark scales and leaf fragments of 1200-1275 CE, or early in the *Hemish* occupation. The cumulic soil development supports the assumptions necessary for modeling accumulation as more or less continuous over the last 5000 years with preceding hiatuses at ~ 6.5, 8.3, 9.5, and 12.5 ka BP before that (Fig. S3 and S4). Charcoal concentrations are at their highest value in late Holocene soils (A1 and A2 horizons) with peak values achieved in the upper portion of the A1 horizon, coincident with *Hemish* occupation and land use in the uplands. Archaeological evidence for agricultural use (field houses and field features) are present within a few hundred meters of the BBO 1 crater, including on the rim of the crater.

Pollen (Fig. S5) and lipid biomarkers (Fig S6) are best preserved for the upper meter of the BBO 1 cores. Below 1 m, pollen sums never exceeded five grains before 300 *Lycopodium* tracers were counted. Below 1 m, stanol concentrations never exceeded 3000 mV*s g^{-1}. Pollen and lipid concentrations were abundant for the last 2000 years, however, with pollen sums between 50-200 grains and stanols largely > 3000 mV*s g^{-1}. Pollen results for the entire core can be found in Fig. S5.

Herbivore fecal stanols and the coprophilus dung fungus *Sporomiella* follow similar patterns of abundance for the upper 1 m of the BBO 1 core (Fig. S6). Peaks in both at the top of the A2 horizon indicate abundant herbivore populations ~ 200-500 cal CE, before the major

Ancestral Jemez occupation in the uplands. A second coincident spike in both proxies in the middle of the A1 horizon indicate abundant herbivore populations coincident with the earliest *Hemish* occupation in the uplands. Both proxies decline during peak Hemish occupation but reach peaks again at the very top of the core. This uppermost spike in herbivore proxies is probably indicative of the increase in domestic herbivores in the 19th century (27).

Banco Bonito 2 (BBO 2). Banco Bonito locality 2 (BBO 2) is a coring location within a ~20 m deep, steep-sided explosion pit on the Banco Bonito Rhyolite (Fig. S1). Vegetation surrounding BBO 2 and its drainage area is almost exclusively ponderosa pine forest, although a small patch of aspen and mixed conifer vegetation is present on the north facing slope of the south end of the explosion pit. Unlike BBO 1, BBO2 has three ephemeral drainage channels that contribute sediment to the basin, draining an area of 115.3 ha, all of which is on the Banco Bonito Rhyolite. This increased sediment supply from alluvial sources has generated a much faster sedimentation rate and a better sorted sediment supply to the BBO 2 cores, which were located in the east-west center of the basin but to the south of a visible alluvial fan entering from the north end of the explosion pit. Because of the enhanced sedimentation rate, despite coring to the maximum depth possible with our equipment (6.4 m of down hole depth) we were unable to reach the bottom of this sequence. All of the sediments extracted were loamy to sandy loam sheetwash alluvium (Table S3; Lithostratigraphic Unit I). Stratigraphic descriptions (Table S3), radiocarbon dates (Table S4), and the age-depth model (Fig. S7) can be found below.

There were six weakly separated immature soils formed in these alluvial sediments over the last 6.5 ka cal BP (Fig. S7; Table S4). This sequence is roughly contemporaneous to the formation of A1, A2, A3, Ab1, Ab2, and Ab3 at BBO 1. Weakly expressed buried soils indicate periods of stability at ~1400 cal CE, 700 cal CE, 600 cal BCE, 800 cal BCE, 1600 cal BCE, and 4000 cal BCE spanning the middle and late Holocene. Charcoal is generally abundant throughout the BBO 2 sequence (as it is in contemporaneous soils at BBO 1) but is at peak values at the very top of the Ab2 soil and in the Ab1 soil. The Ab1 soil clearly dates to the early Hemish occupation (Fig. S8 and Table S4) and age-depth modeling (Fig. S7) projects peak charcoal concentrations for the earliest occupation followed by a second peak immediately after depopulation (in the modern A horizon). Abundant charcoal in the surface sample is partly an artifact of abundant charcoal on the surface after a prescribed burn the year prior to sampling. Although deposition is not continuous at BBO 2, where dated directly the hiatuses represented by each buried surface may be as little as one to three centuries, suggesting that continuous age-depth modeling provides a useful proxy for variability in charcoal deposition. Archaeological evidence for agricultural use (field houses and field features) are present within a few hundred meters of the BBO 2 crater, including on the rim of the crater itself.

[Pollen section (Fig S9)] Pollen concentrations were highest in the upper 80 cm of the cores. Full pollen data can be found in Fig. S9.

Cebollita Springs 3 (CBS 3). Cebollita Springs 3 (CBS 3) is a coring location in an alluviated valley with a Bandelier Tuff bedrock basement that creates a (now enclosed and modified) spring (Figs. S10 and S11). Vegetation on the slopes surrounding the coring location and the upslope drainage basin is exclusively ponderosa pine forest. The 391.3 ha drainage basin drains an area of both Otowi and Tshirege members of the Bandelier Tuff. There is no channel in the valley here today. Four 320 cm cores were retrieved approximately 15m from a fenceline enclosing the modified spring and yielded sediments that indicate that both overland flow and spring activity were greater in the past. Stratigraphic descriptions (Table S5), radiocarbon dates (Table S6), and the age-depth model (Fig. S12) can be found below.

Unlike the more or less continuous deposition in the BBO 1 and BBO 2 basins, sedimentation at CBS 3 was clearly episodic and discontinuous (Figs. S12 and S13). At CBS 3, at least three relatively stable wet meadow soils are stratified within alternating upward fining beds that grade from coarse, angular, unsorted gravely muds capped with fine-grained, organic and charcoal rich A horizons spanning the last 5.5 ka cal BP. Charcoal is abundant in both the gravelly muds (colluvium deposited in a wet meadow) and the fine-grained wet meadow soils but is most abundant in the slowly accumulating wetland 5Ab2 soil and again in the rapidly accumulating A and 3Ab1 soils. The uppermost 110 cm disclosed two rapidly accumulating

upward fining sets that date between roughly 1200-1400 cal CE, or the earliest phases of *Hemish* occupation and population growth. This is the most rapid sedimentation in the sequence (Fig. 12) and suggests that both fire activity and erosion within the basin were enhanced to peak late Holocene levels with the establishment and expansion of the *Hemish* agricultural landscape. Archaeological evidence for agricultural use (field houses and field features) are present within the CBS 3 watershed, including a field house within 200m of the coring location.

Pollen was relatively well preserved in the wet meadow soils, but the surface sample should be considered as a palimpsest of deposition since the late 1300s. This surface sample was not considered in the *Sporormiella* representation because the valley is actively grazed by cattle now and the high concentrations of the dung fungus in this sample is probably due to recent and historic pastoralism. Full pollen data can be found in Fig. S14.

Lake Fork Canyon 3 (LFC 3B and 3C). Lake Fork Canyon 3 includes two coring locations with one core at each spot (LFC 3B and 3C). LFC 3 has a 1303 ha drainage area entirely within the Tshirege member of the Bandelier Tuff (Fig. S10). The canyon is an east-west trending grass dominated valley with ponderosa pine forests covering the south facing slopes on the north side of the valley and mixed conifer vegetation on the steep, north facing slope on the south side of the valley (Fig. S15) although ponderosa pine forests also cover the mesas above the belt of mixed conifer to the south. The LFC 3 locality is a groundwater supported, sedge covered bog with essentially no open water today (Fig. S15). Overland flow within the large drainage basin potentially contributes sediment to the bog but the abundance of sedge limits that transport to the center of the bog, meaning that most sedimentation is primarily from *in situ* organic deposition and eolian contributions with a very slow overall sedimentation rate. The LFC 3B core spot was near the north margin of the bog, about 20 m from the south facing slope. The LFC 3C core spot was from the center of the bog (relative to the north and south margins) but towards the upstream end of the bog. LFC 3C was approximately 50 m from the LFC 3B core spot. Stratigraphic descriptions (Table S7), Pb-210 age estimates (Table S8), radiocarbon dates (Tables S9 and S10), and age-depth models (Figs. S16 and S17) can be found below. Pb-210 ages were problematic at Alamo Bog and were not included in the age model there (28). Pb-210 ages were also problematic at the LFC bog and were mostly not included in the age model here (Table S8).

Despite the physical distance between the two cores and the proximity of the LFC 3B core to the south facing slope, the general stratigraphy of the cores is similar, suggesting that the sediment sources at both are predominantly local and eolian, although hillslope derived inorganic sediments are clearly more abundant at LFC 3B. The base of the 3B core was a 5.5 ka cal BP soil that was probably a terrestrial surface when Middle Holocene aridity shrunk the surface area of the bog. This stratigraphic unit was not encountered in the LFC 3C core. Lithostratigraphic Unit II was characterized by interbedded peats and muds dating to between ~1 – 4 ka cal BP. Lithostratigraphic Unit III dates to the period of peak Hemish occupation and is characterized by increased inorganic sedimentation and much higher sedimentation rates, suggesting an increased sediment supply. Lithostratigraphic Unit IV is characterized by much slower organic sedimentation to the modern surface of the bog.

Charcoal concentrations are abundant at both localities, although concentrations are generally lower in the rapidly accumulating Unit III, the rapid sedimentation rates here mean that charcoal accumulation rates are actually the highest on record during this time. This period of rapid sedimentation is accompanied by an increase in the abundance of old, reworked pieces of charcoal that are rejected from the age-depth model. Importantly, Unit III at both localities clearly dates to the early centuries of Hemish occupation, suggesting that the establishment and expansion of the agricultural landscape involved increased fire activity and enhanced erosion. Following the example by Allen and others (28), we compared charcoal variability between the 3B and 3C cores (Fig. S18). Despite subtle differences in sedimentation the two cores, the general patterns of macroscopic charcoal concentrations are similar, with comparable peaks across initial *Hemish* settlement and again at the end of occupation or immediately after depopulation of upland villages (ca. 1600-1650 cal CE). Archaeological evidence for agricultural use (field houses, field features, and small settlements) are present within a few hundred meters of the LFC watershed.

Pollen was well preserved and abundant throughout the LFC 3C core, although pollen concentrations were generally lower during the period of rapid inorganic sedimentation between 20-40 cm (1100s CE). Full pollen data can be found in Fig. S19.

Monument Canyon 4 (MCA 4 and 4B). Monument Canyon locality 4 (MCA 4 and MCA 4B) is a trenching location within the upstream reach of the drainages below the Monument Canyon Research Natural Area (Fig. S20). Vegetation on the uplands surrounding MCA 4 are ponderosa pine forests, whereas in the narrow drainage, Douglas fir and white fir, mostly less than 100 years old, are common (Fig. S21). The 192 ha drainage area mostly drains areas of the Bandelier Tuff (both Otowi and Tshirege members) as well as a small area of El Cajete Pumice. The original trench at MCA 4 exposed a complex superposition of Middle Holocene aged alluvium and debris flows, a late Holocene channel and channel fill, followed by late Holocene alluvial channel fan deposits (Fig. S22). We will only discuss the late Holocene stratigraphy here. In 2014, extensive erosion and channel expansion exposed a broad stretch of the alluvial channel fan deposits at MCA 4. A second sampling column was collected at MCA 4B to assess reproducibility of the charcoal record from MCA 4 strata (Fig. S23). Stratigraphic descriptions (Table S11), radiocarbon dates (Table S12), and the age-depth model (Fig. S24) can be found below.

The late Holocene stratigraphic sequence at MCA 4 is less than 1.5 m thick, but it includes two major charcoal beds that are interstratified with fine-grained alluvium over well sorted channel deposits (Lithostratigraphic Unit IV) (Figs. S22 and S25). Radiocarbon dates indicate that channel fan and overbank deposits began accumulating by the 1200s cal CE (Fig. S25 and Table S12). A pith date of a ponderosa pine tree growing on the surface of the fan terrace in which MCA 4 and 4B are located indicate that sedimentation had to have ceased by 1714 CE. Using this *terminus ante quem* tree-ring age, radiocarbon dated charcoal from the charcoal beds indicate that these formed between 1650-1700 cal CE or the decades immediately after the depopulation of the major villages in the uplands. Although the A horizon deposits were slightly thicker at MCA 4B, the general pattern of charcoal abundance is comparable for the two profiles with a 10 cm offset to account for this. Abundant quality-controlled tree-ring samples document frequent low-severity surface fires in this watershed from at least 1650 CE onward.

The MCA 4 watershed has numerous archaeological sites indicative of agricultural use (field houses and field features). Charcoal concentrations were relatively low (compared to the dense charcoal layers in 2C2, 2C3, and 2C4) during *Hemish* occupation and land use, although the lower values for MCA 4 in 2C5 and 3C may be due to differential settling in sandier facies than at 4B, which had higher charcoal concentrations and finer textured sediments from these deposits.

Pollen was abundant above 60 cm at MCA 4, in the sediments that post-date Hemish occupation. Full pollen data can be found in Fig. S26.

Upper San Juan Canyon 2 (SJC 2). Upper San Juan Canyon locality 2 (SJC 2) was a coring locality on an isolated alluvial terrace on the north side of Cerro del Pino (Fig. S27). The 1318.7 ha drainage area above the SJC 2 coring locality includes complex Quaternary and Tertiary volcanics, including Paliza Canyon formation dacite, rhyodacite, quartz lattite, and andesites, the Bearhead rhyolites, and the El Cajete Pumice. Vegetation around the coring locality is predominantly ponderosa pine forest but mixed conifer stands cover the northeast facing slope of Cerro del Pino to the southwest of the alluvial terrace, and very young white fir and Douglas fir are filling in the ponderosa forest within the valley (Fig. S28). Stratigraphic descriptions (Table S13), radiocarbon dates (Table S14), and the age-depth model (Fig. S29) can be found below.

The SJC 2 cores refused on coarse channel lag and revealed a fairly uniform sequence of loamy overbank alluvial deposits (Fig. S30). There was a hiatus in accumulation from ~200-1400 cal CE but rapid sedimentation continued between roughly 1400-1650 CE. These deposits created a 155 cm thick cumulic A horizon with abundant charcoal. A short-lived paleosurface that was welded into the cumulic soil may have existed at ~80-90 cm but this was not visibly evident in the cores nor is it evident in the chronostratigraphy. Rather, this cumulic soil, which dates exclusively to the period of peak *Hemish* occupation and land use, indicates abundant hillslope erosion and fire activity from an area that is conventionally considered to be outside of the most intensive agricultural use. There is no archaeological evidence for use of the SJC 2 watershed,

although there is archaeology downstream on the mesas surrounding San Juan Canyon. However, the increased sedimentation and charcoal deposition during peak Hemish populations is further evidence of the expanding impact of Native American fire management on the larger landscape, as seen in the modeling and tree-ring evidence.

The FireBGCv2 model

The Fire BGCv2 model operates across hierarchical spatial scales from 1) fixed-boundary biophysical sites, 2) dynamic stands defined by vegetation composition and structure, 3) simulation plots on which ecosystem processes are modeled for computational efficiency, 4) tree species and understory plant guilds, to 5) individual trees with attributes such as species, age, height, diameter at breast height (DBH), and leaf area. In the model climate, wildland fire, and landscape vegetation are dynamically and reciprocally linked: long-term records of daily temperature, precipitation, and radiation influence fuel production and moisture, which determine landscape ignition potential, fire frequency and size, and fire behavior. Climate and weather influence the productivity and mortality rates of individual plant species - and thus stand composition and structure - with feedbacks to the fire regime via fuel type, fuel amount, and fuel arrangement. Fire regimes in turn affect vegetation species' regeneration, composition, successional trajectories, and productivity directly through fire-caused mortality and successional patterns, and indirectly through influence on availability of light, water and other necessary resources. Required model inputs are site and stand maps, daily weather, fire frequency and size parameters, species parameters that dictate phenology, establishment, growth, and mortality, and initializing stand data for representative vegetation communities.

Wildland fire ignitions (lightning-caused) are simulated across sites using functions that relate the Keetch-Byram Drought Index (KBDI) to parameterized fire return intervals (29). Climate and weather influences on fire ignitions are accounted for using daily deviations of site-level KBDI from an average maximum fire season KBDI, where probability of fire increases as conditions become drier. Fires spread across the simulation landscape via cell percolation following slope gradients and wind direction. Fire spread is terminated when fuels are too wet or too sparse or when cumulative annual area burned reaches an area stochastically determined from input average fire size. Potential fire sizes are scaled to KBDI – hot, dry conditions increase the occurrence probability of large fires – but actual fire sizes are constrained by fuel availability and moisture.

Individual tree mortality occurs as the result of wildfire damage, hydrologic stress, crowding, light reduction, and random mortality. Fire-caused tree mortality is modeled as a function of bark thickness (a user-defined, species-specific parameter) and scorch height, and can be used to assess fire severity where the degree of crown scorch and cambial kill depends on fire intensity and duration. Thermal limits are defined for each species in the model according to parameterized minimum, maximum, and optimal growing degree days, where temperatures outside of these limits affect trees through a reduction in the annual growth increment and eventual mortality. Tree regeneration is driven by soil moisture, litter depth, and climate-influenced cone crop production.

Required model inputs are ecological site and stand maps, daily weather for ecological sites, fire regime and vegetation parameters, and initializing stand (plot) vegetation and fuels data. Ecological sites (ponderosa pine, 61,451 ha; wet mixed conifer, 60,795 ha; piñon-juniper, 41,009 ha; dry mixed conifer, 16,039 ha; and riparian, 1824 ha) were mapped from the LANDFIRE environmental site potential (ESP) data layer (30), resampled to 90m, and generalized based on nearest neighbors to reduce fine-scale heterogeneity. Initial stand boundaries were defined using the LANDFIRE biophysical settings layer, and plot data from 84 plots collected across the Jemez landscape in 2012-2013 (for detailed field methods see Clark et al. (31) and Loehman et al. (32)) or obtained from the Forest Inventory and Analysis Program (http://www.fia.fs.fed.us/) were assigned to stands based on similarities of dominant species, elevation, slope, and aspect. Weather data were obtained from the Jemez Springs National Climatic Data Center cooperative weather station (CO-OP ID 294369-2) and were extrapolated across sites (33). Historical fire frequency and size distributions were derived from fire history studies for southwestern ecosystems (34-37), including local studies (38, 39). Vegetation species parameters were gleaned from literature, previous FireBGCv2 projects (31, 32), and field data.

We adjusted fire size and frequency parameters until the model simulated landscape fire return intervals that were consistent with available fire history records. We adjusted biological tree species parameters (e.g., shade tolerance, growing degree days, cone crop probability, bark thickness) until modeled spatial distributions and individual species basal area characteristics matched published estimates for southwest vegetation communities under non-managed conditions (e.g., without suppression, logging, or other activities) (40-43).

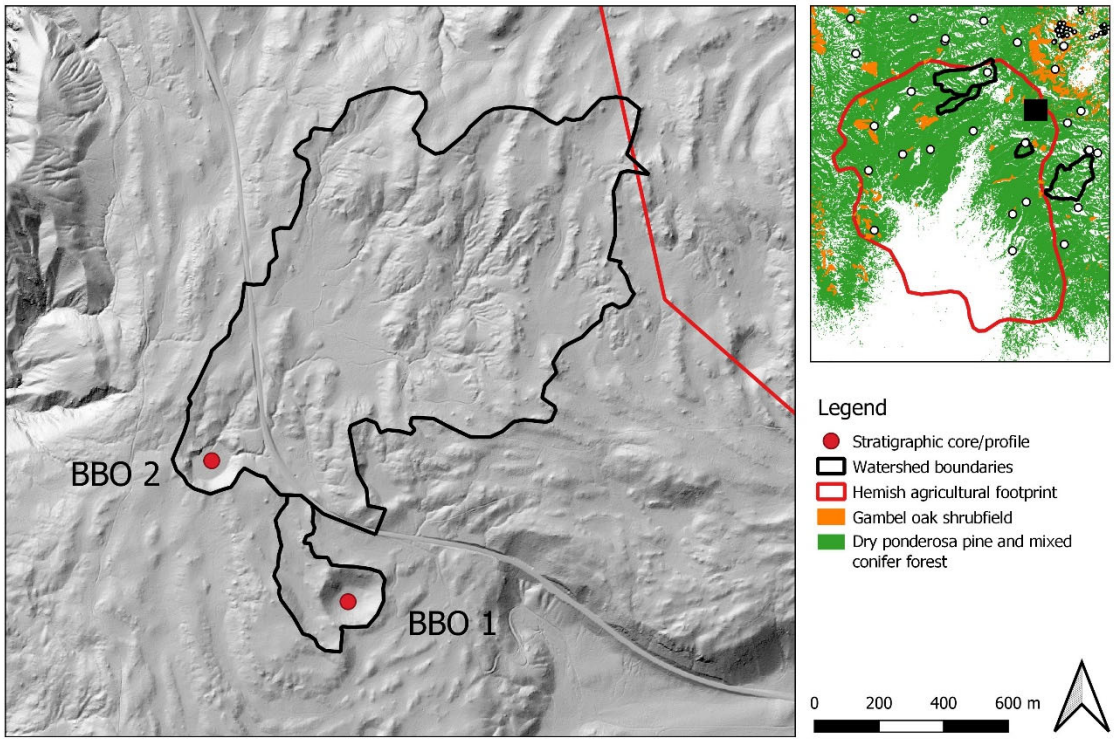

Fig. S1. Topographic map of the watershed catchments for the two coring localities on the Banco Bonito rhyolite flow (BBO 1 and BBO 2). Scale apples to primary map tile on the left. Hillshade is from bare-earth LiDAR data provided by the Southwest Jemez Community Forest Landscape Restoration project.

Fig. S2. Landscape context of coring at the bottom of an explosion pit on the Banco Bonito rhyolite flow (BBO 1 in this case). View is to the southwest. (Photo by A. Steffen.)

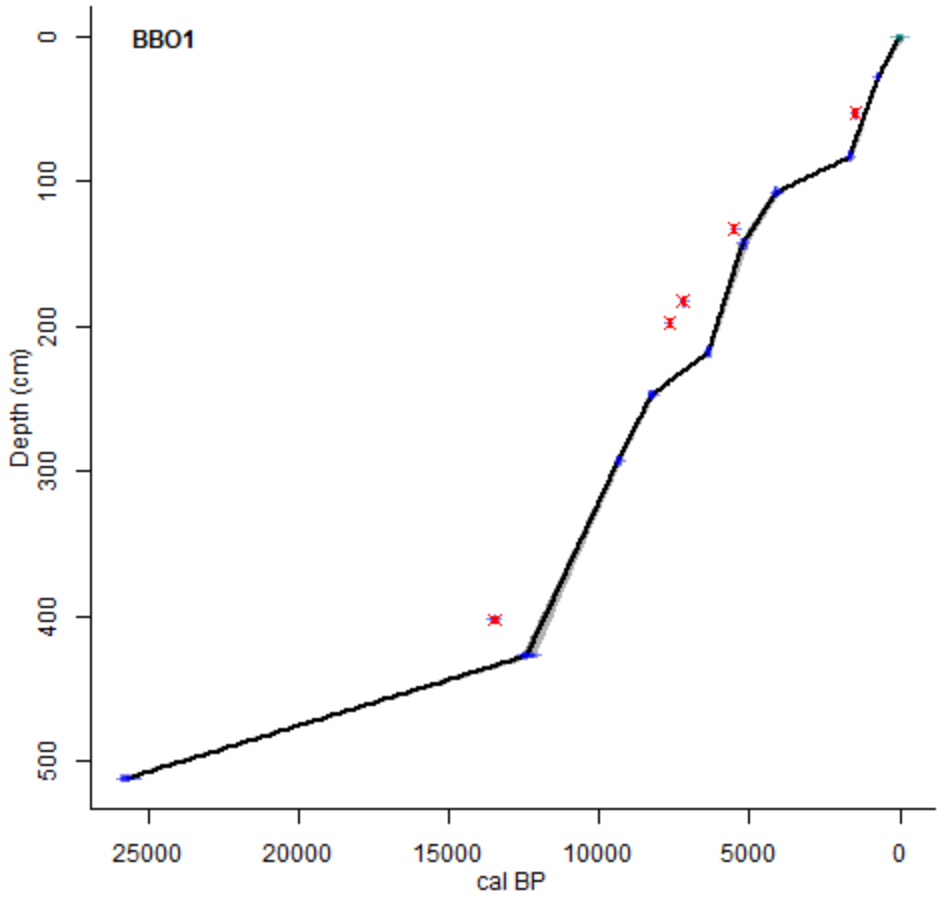

Fig. S3. Age-depth model from for the BBO 1 core. Red bars indicate 2σ calibrated age ranges of old or reworked charcoal ages that were excluded from the model. Blue bars indicate 2σ calibrated age ranges of charcoal dates that were included from the model.

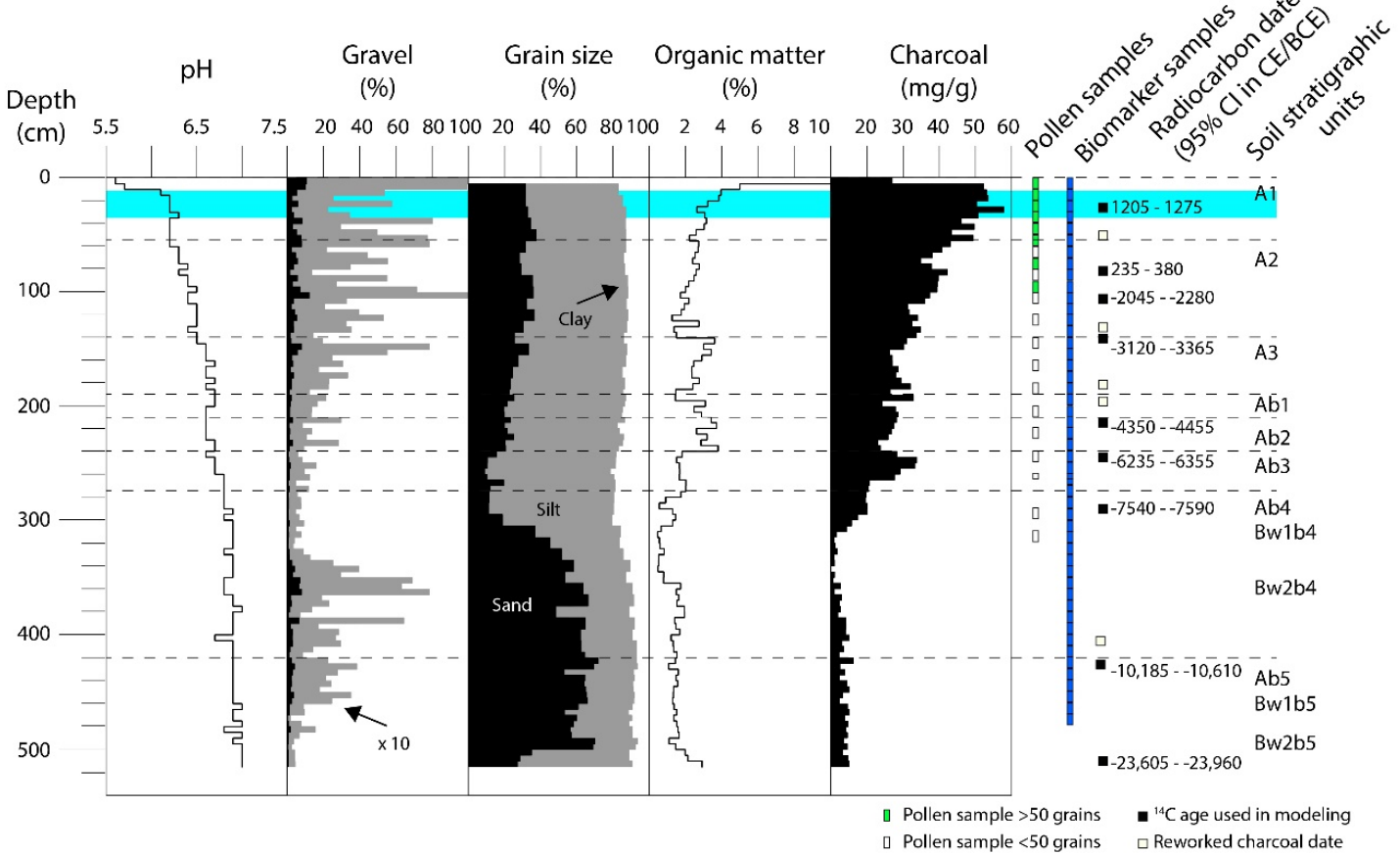

Fig. S4. Stratigraphic plot of pH, gravel, grain size distributions, organic matter, and charcoal concentrations for BBO 1. Also indicated are the soil horizons and the location of pollen and lipid biomarker samples and radiocarbon dates used in the age model. The turquoise zone is the depth range that the age-model includes within the Hemish occupation (ca. 1100-1650 CE).

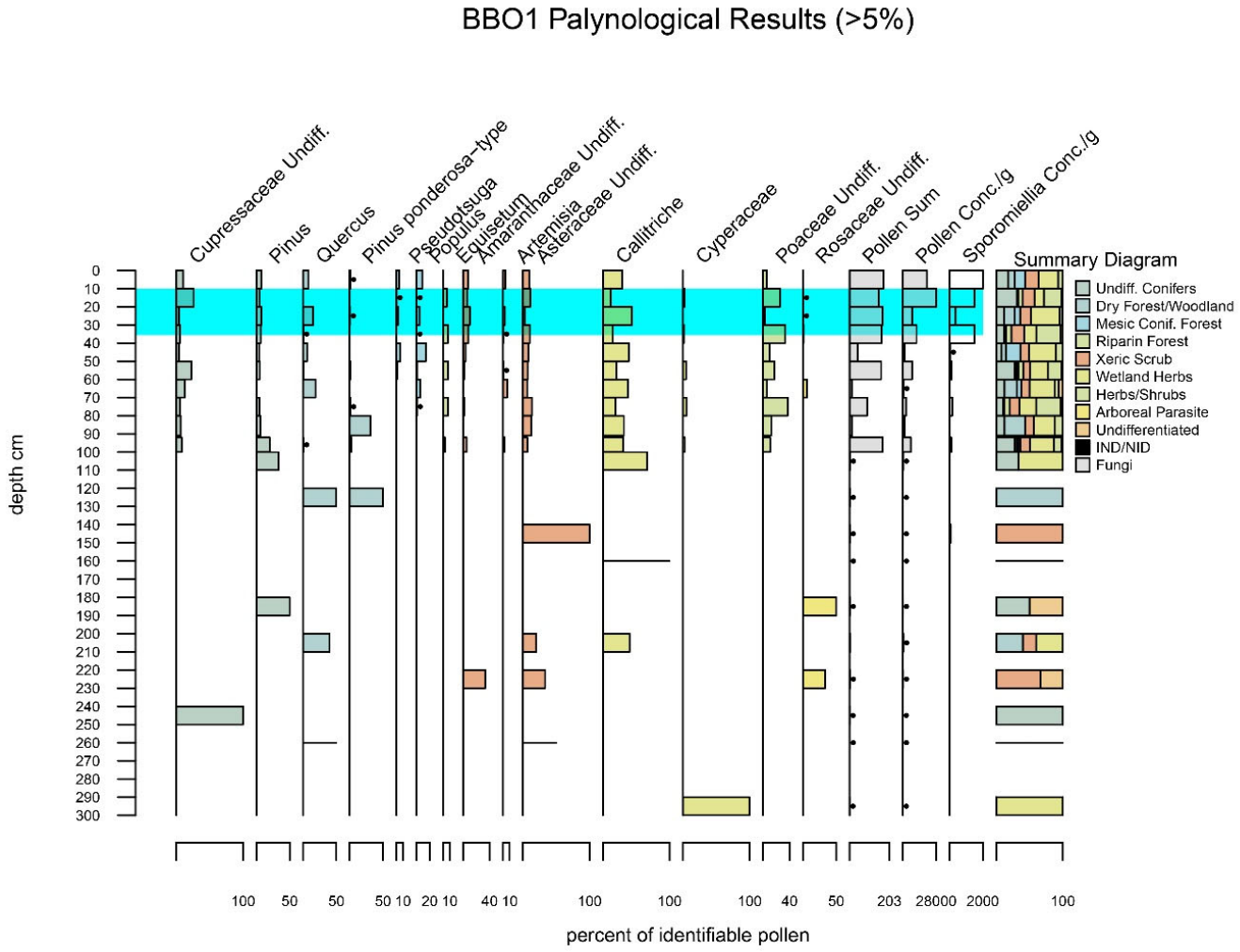

Fig. S5. Stratigraphic plot of pollen percentages for BBO 1 showing only those pollen taxa that reach at least 5% at some point in the profile. The turquoise zone is the depth range that the age-model includes within the Hemish occupation (ca. 1100-1650 CE).

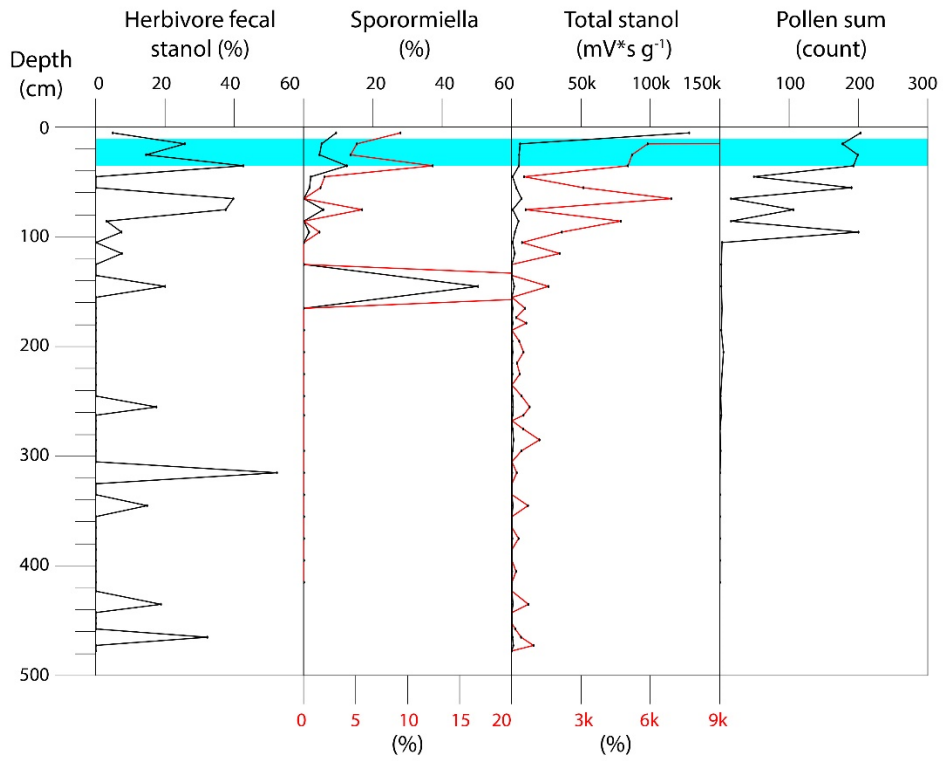

Fig. S6. Stratigraphic plot of herbivore fecal lipid biomarkers (fecal stanols), concentrations of the herbivore dung fungus *Sporormiella*, total stanols, and total identified pollen (pollen sums) from BBO 1. The turquoise zone is the depth range that the age-model includes within the Hemish occupation (ca. 1100-1650 CE).

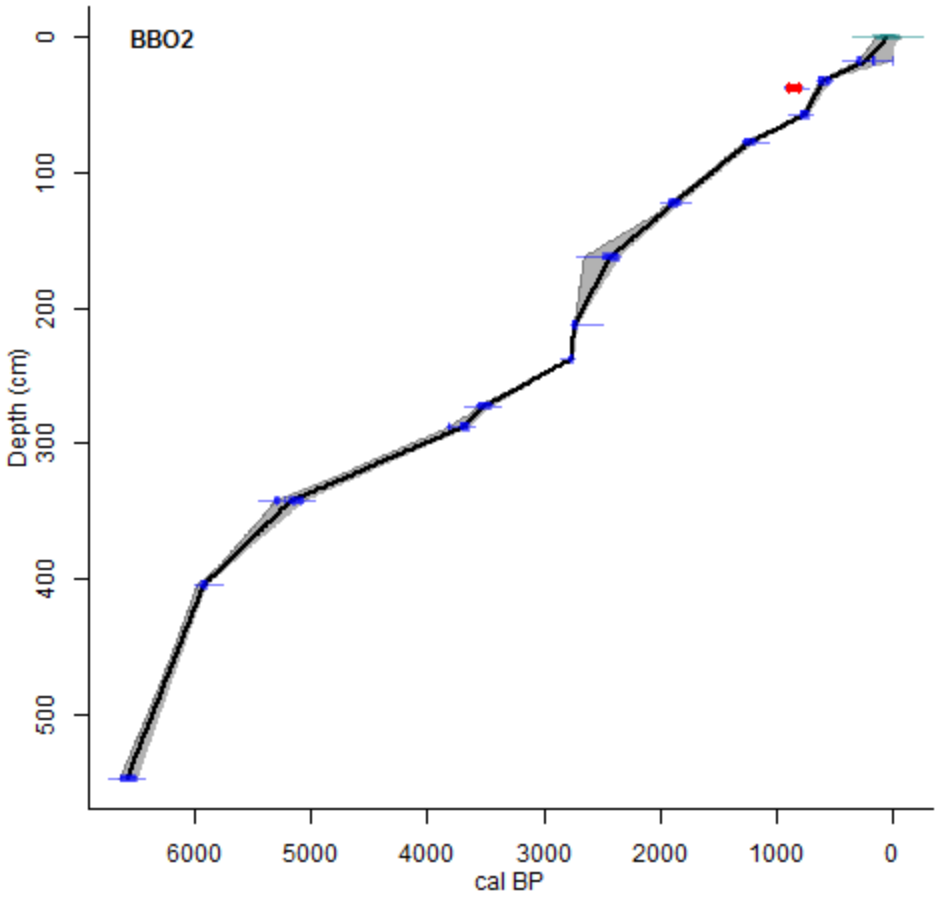

Fig. S7. Age-depth model from for the BBO 2 core. Red bars indicate 2σ calibrated age ranges of old or reworked charcoal ages that were excluded from the model. Blue bars indicate 2σ calibrated age ranges of charcoal dates that were included from the model.

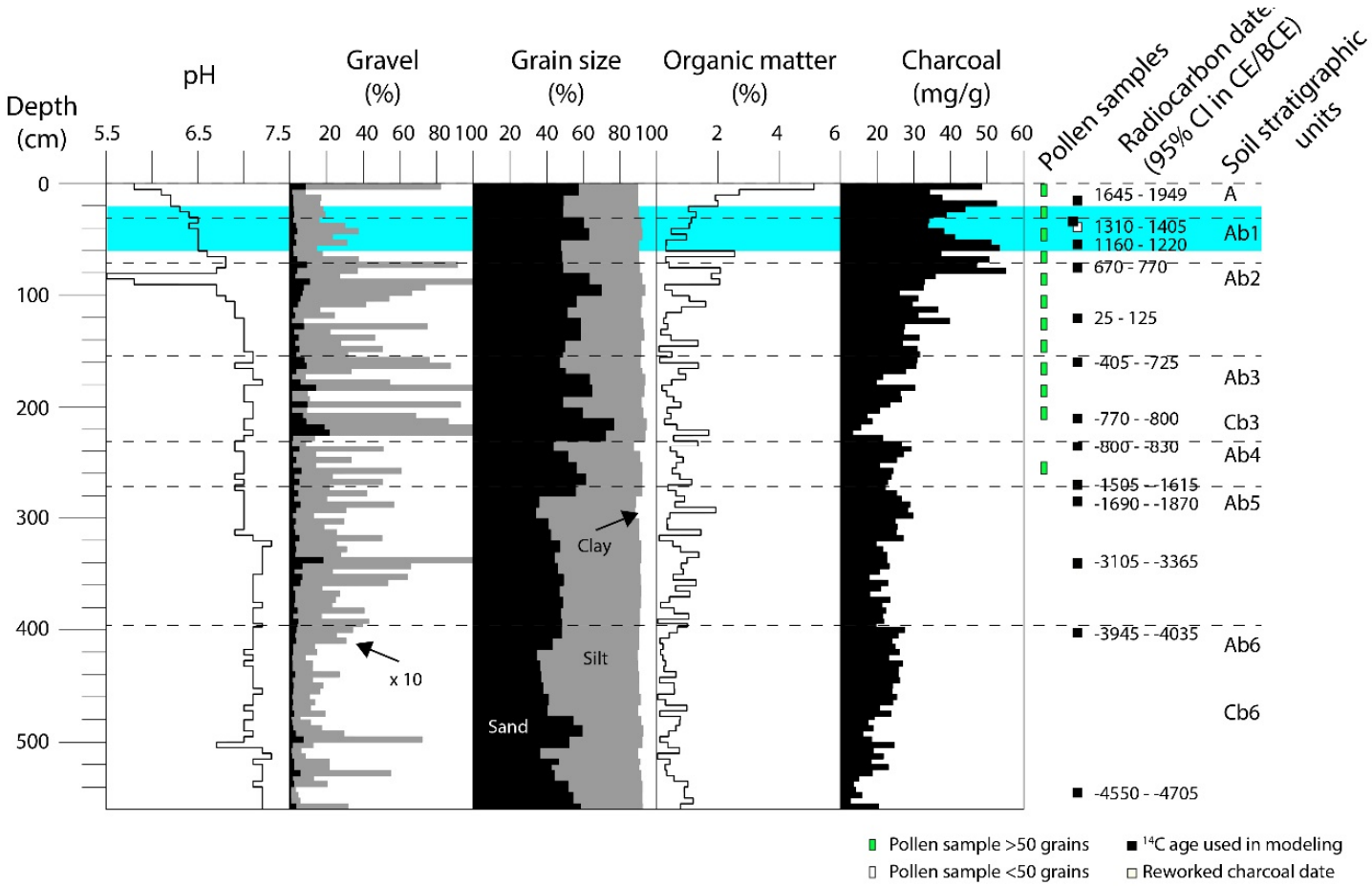

Fig. S8. Stratigraphic plot of pH, gravel, grain size distributions, organic matter, and charcoal concentrations for BBO 2. Also indicated are the soil horizons and the location of pollen samples and radiocarbon dates used in the age model. The turquoise zone is the depth range that the age-model includes within the Hemish occupation (ca. 1100-1650 CE).

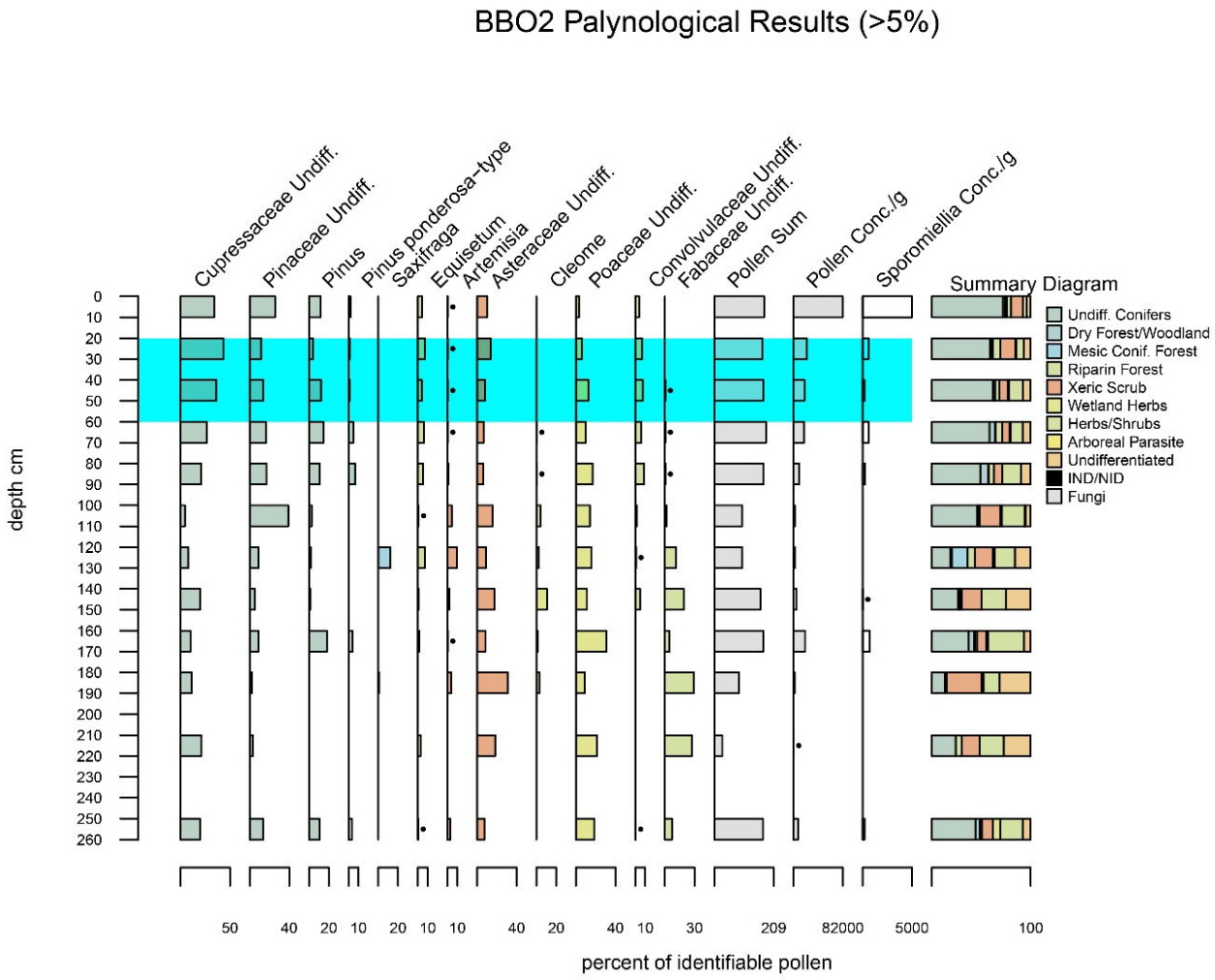

Fig. S9. Stratigraphic plot of pollen percentages for BBO 2 showing only those pollen taxa that reach at least 5% at some point in the profile. The turquoise zone is the depth range that the age-model includes within the Hemish occupation (ca. 1100-1650 CE).

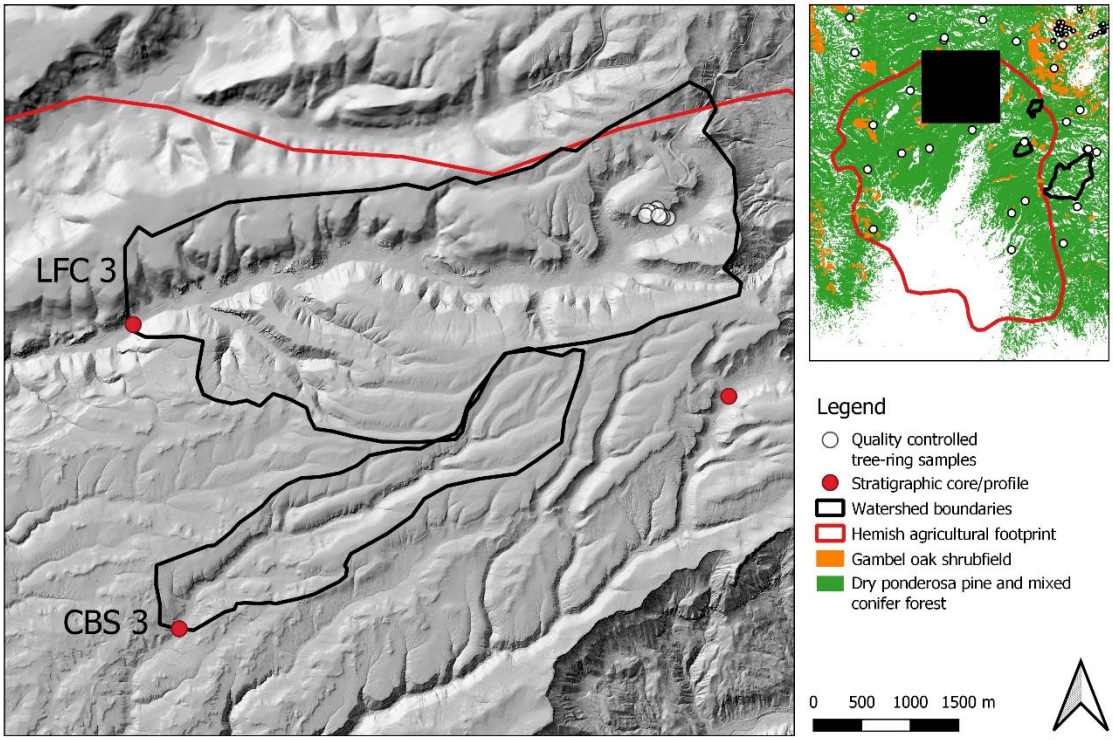

Fig. S10. Topographic map of the watershed catchments for the coring in Lake Fork Canyon (LFC 3C) and Cebollita Springs (CBS 3). Scale apples to primary map tile on the left. Hillshade is from bare-earth LiDAR data provided by the Southwest Jemez Community Forest Landscape Restoration project.

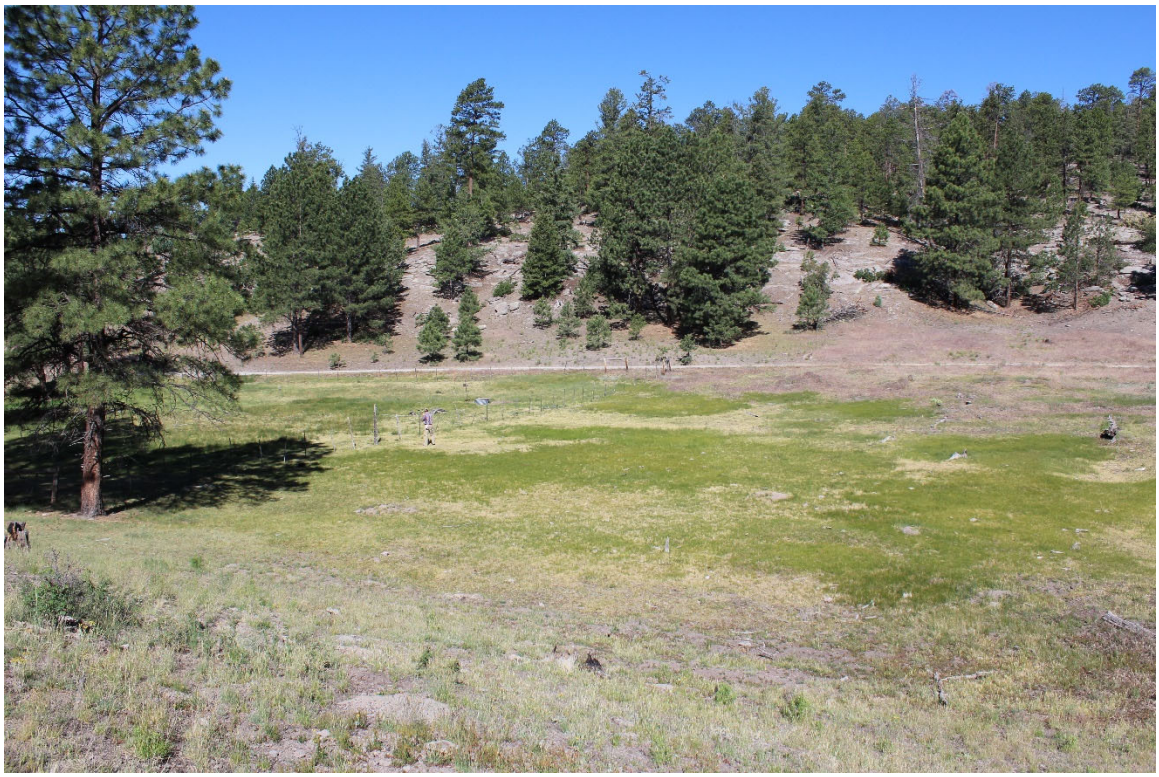

Fig. S11. Landscape context of the coring location at Cebollita Springs (CBS 3). View is to the northwest. (Photo by C. Roos.)

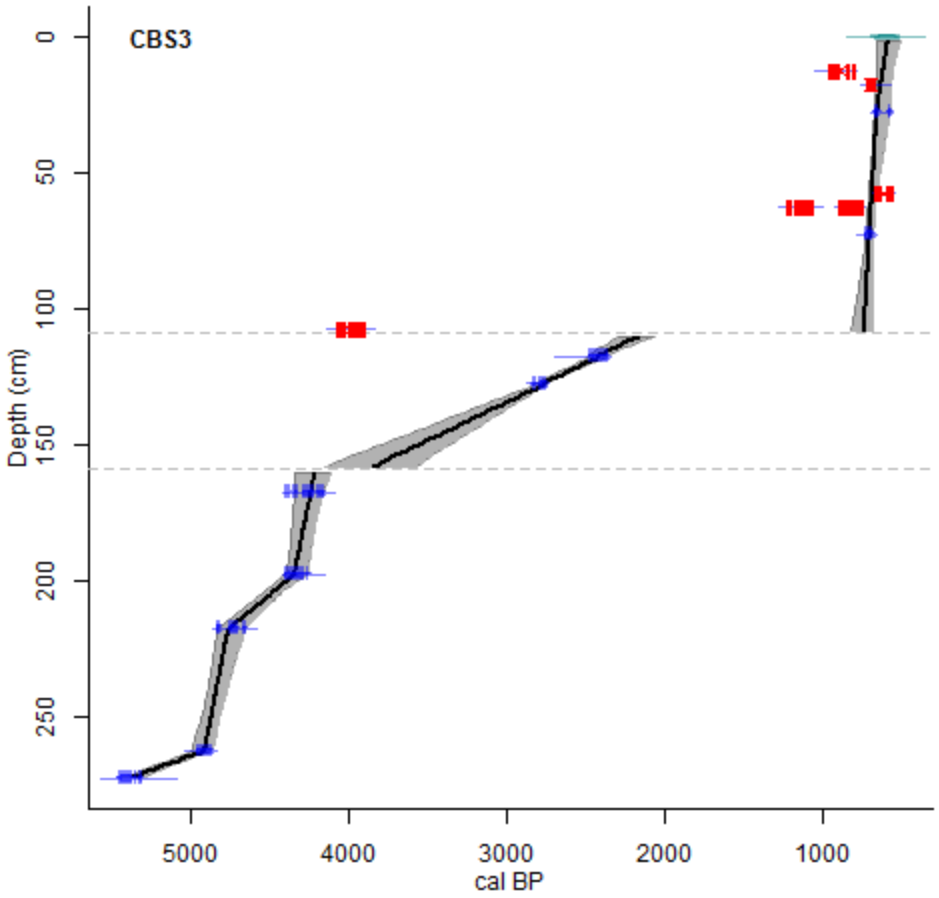

Fig. S12. Age-depth model from for the CBS 3 core. Red bars indicate 2σ calibrated age ranges of old or reworked charcoal ages that were excluded from the model. Blue bars indicate 2σ calibrated age ranges of charcoal dates that were included from the model.

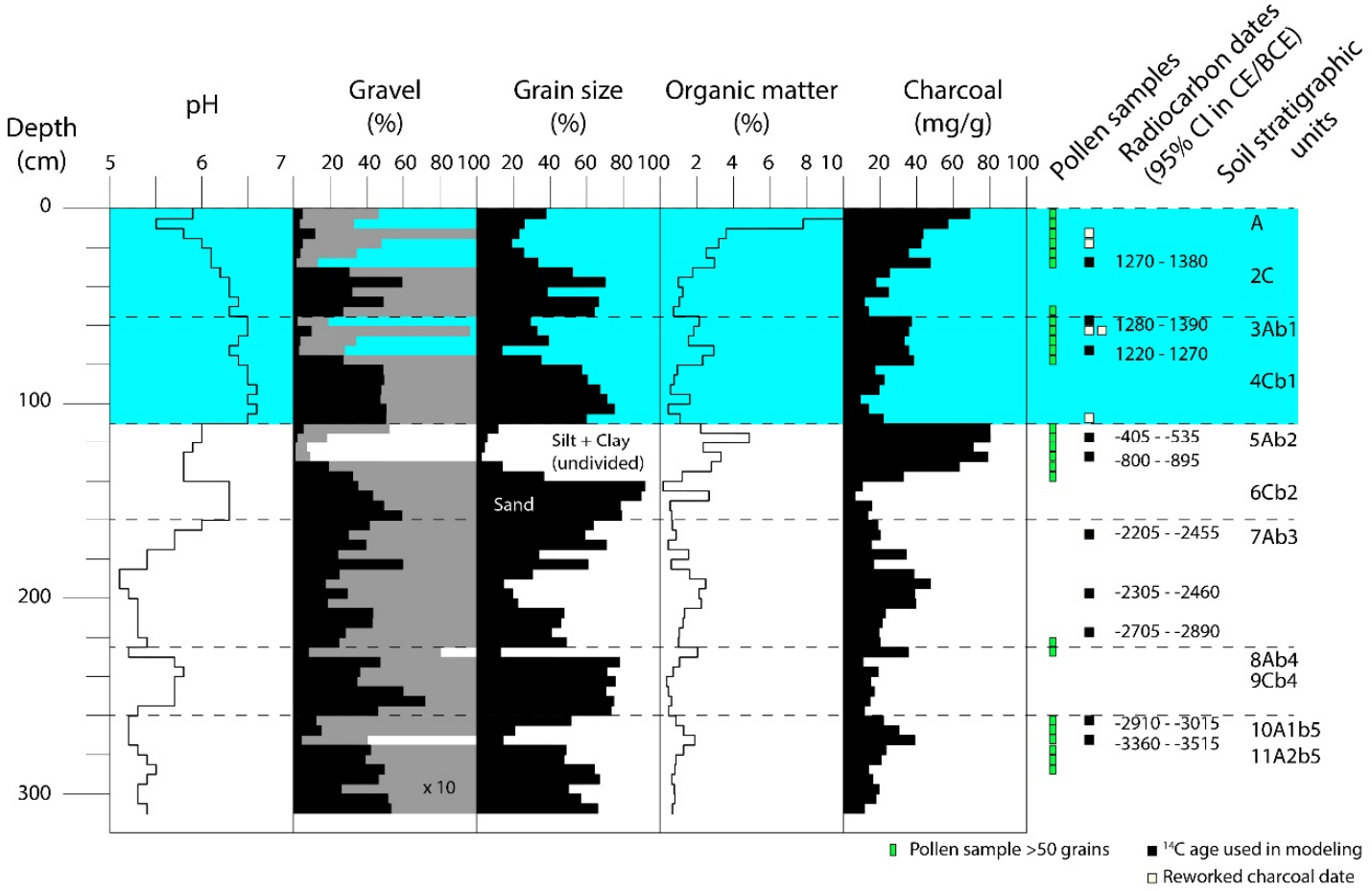

Fig. S13. Stratigraphic plot of pH, gravel, grain size distributions, organic matter, and charcoal concentrations for CBS 3. Also indicated are the soil horizons and the location of pollen samples and radiocarbon dates used in the age model. The turquoise zone is the depth range that the age-model includes within the Hemish occupation (ca. 1100-1650 CE).

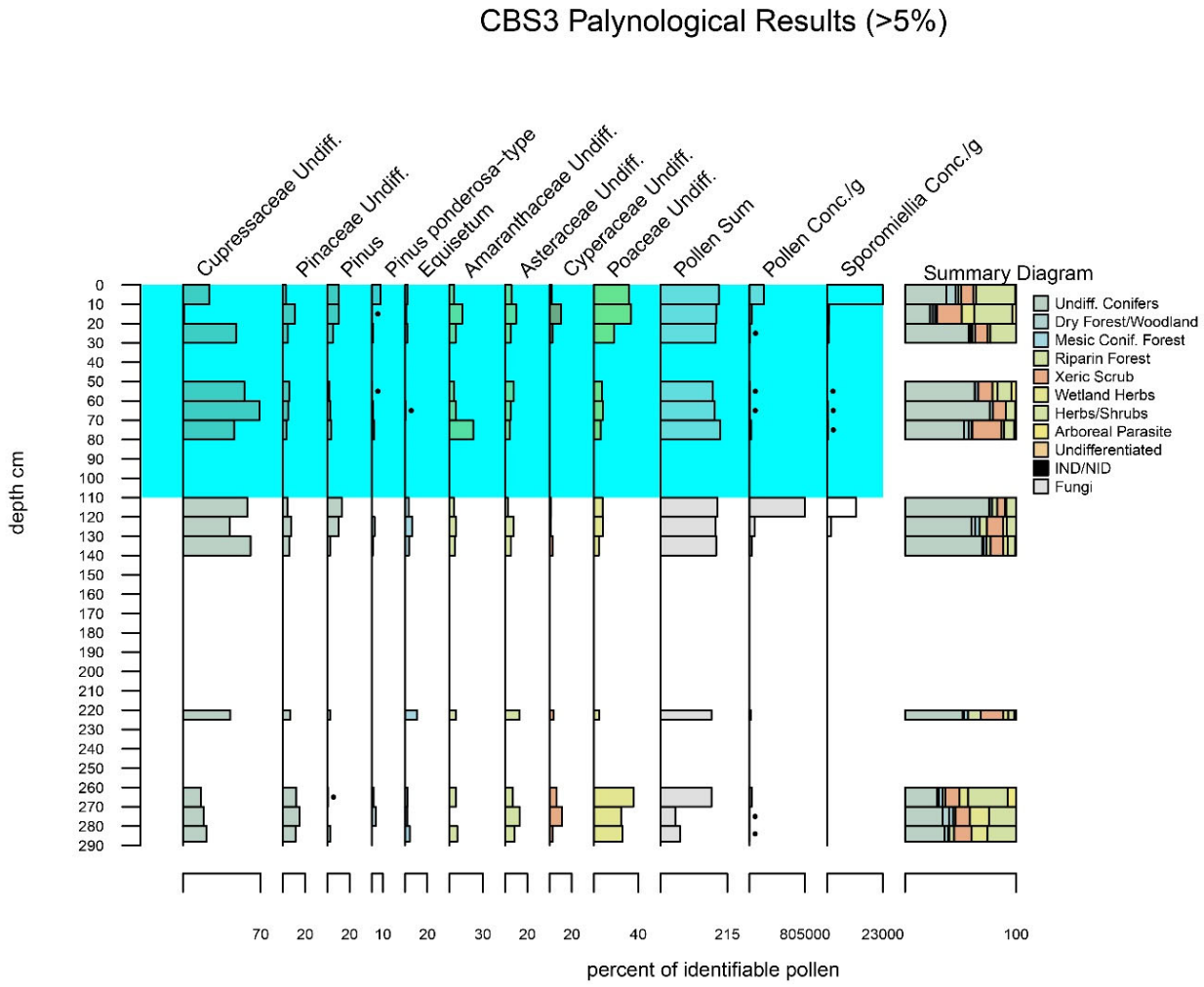

Fig. S14. Stratigraphic plot of pollen percentages for CBS 3 showing only those pollen taxa that reach at least 5% at some point in the profile. The turquoise zone is the depth range that the age-model includes within the Hemish occupation (ca. 1100-1650 CE).

Fig. S15. Landscape context of the coring location at Lake Fork Canyon (LFC 3C and 3B). View is to the west/southwest with mixed conifer forests on the north facing slope (left side of the bog) and ponderosa pine forests on the south facing slope (right of the road). Core 3B was about 15 meters from the edge of the bog in the foreground. Core 3C was from the center of the bog. (Photo by C. Roos.)

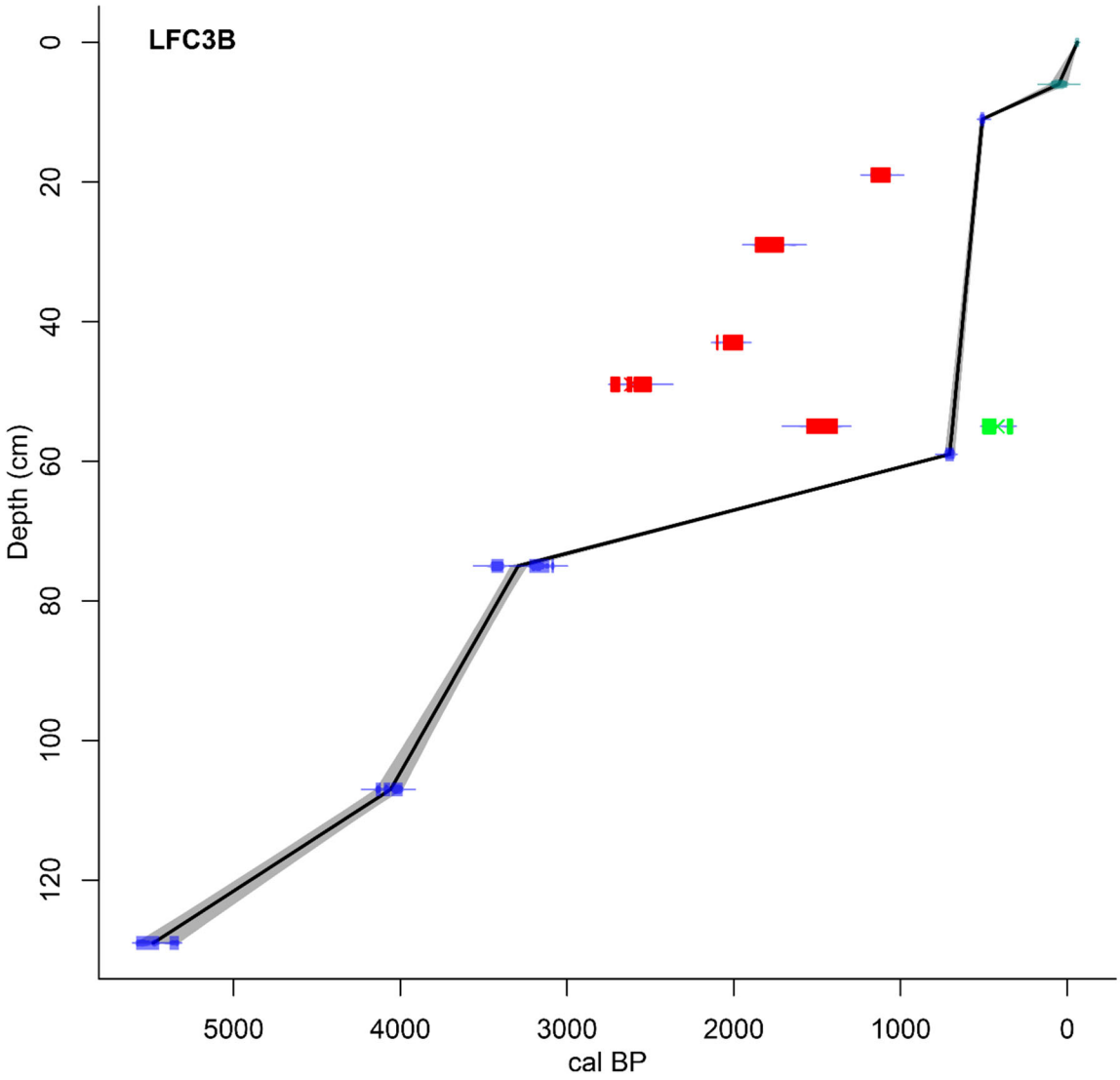

Fig. S16. Age-depth model from for the LFC 3B core. Red bars indicate 2σ calibrated age ranges of old or reworked charcoal ages that were excluded from the model. Blue bars indicate 2σ calibrated age ranges of charcoal dates that were included from the model. Green bar indicates 2σ calibrated age range of unburned organics from the top of a core boundary (contamination).

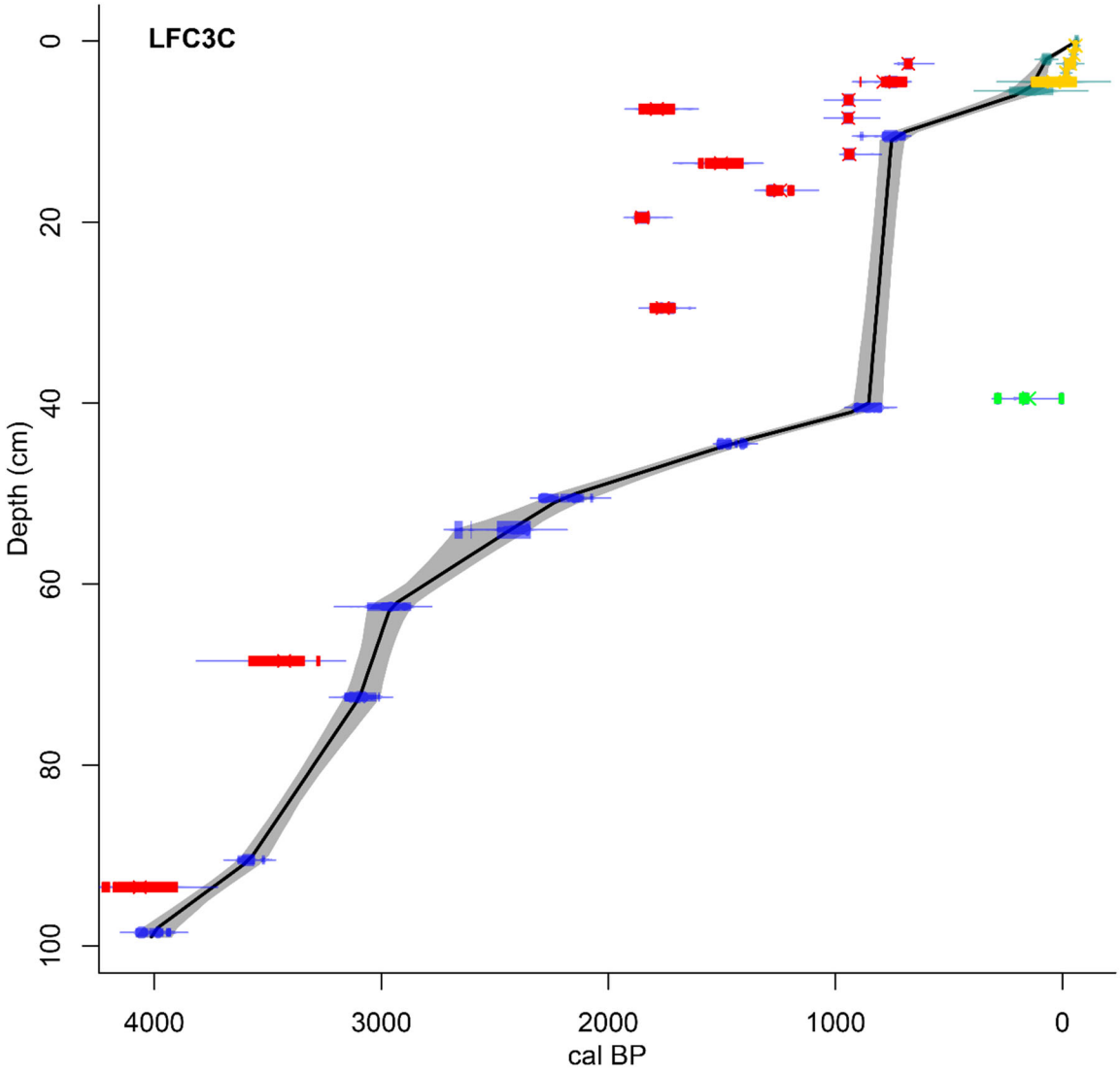

Fig. S17. Age-depth model from for the LFC 3C core. Red bars indicate 2σ calibrated age ranges of old or reworked charcoal ages that were excluded from the model. Blue bars indicate 2σ calibrated age ranges of charcoal dates that were included from the model. Green bar indicates 2σ calibrated age range of unburned organics from the top of a core boundary (contamination). Yellow bars indicate the 2σ Pb-210 age ranges that were excluded from the age model.

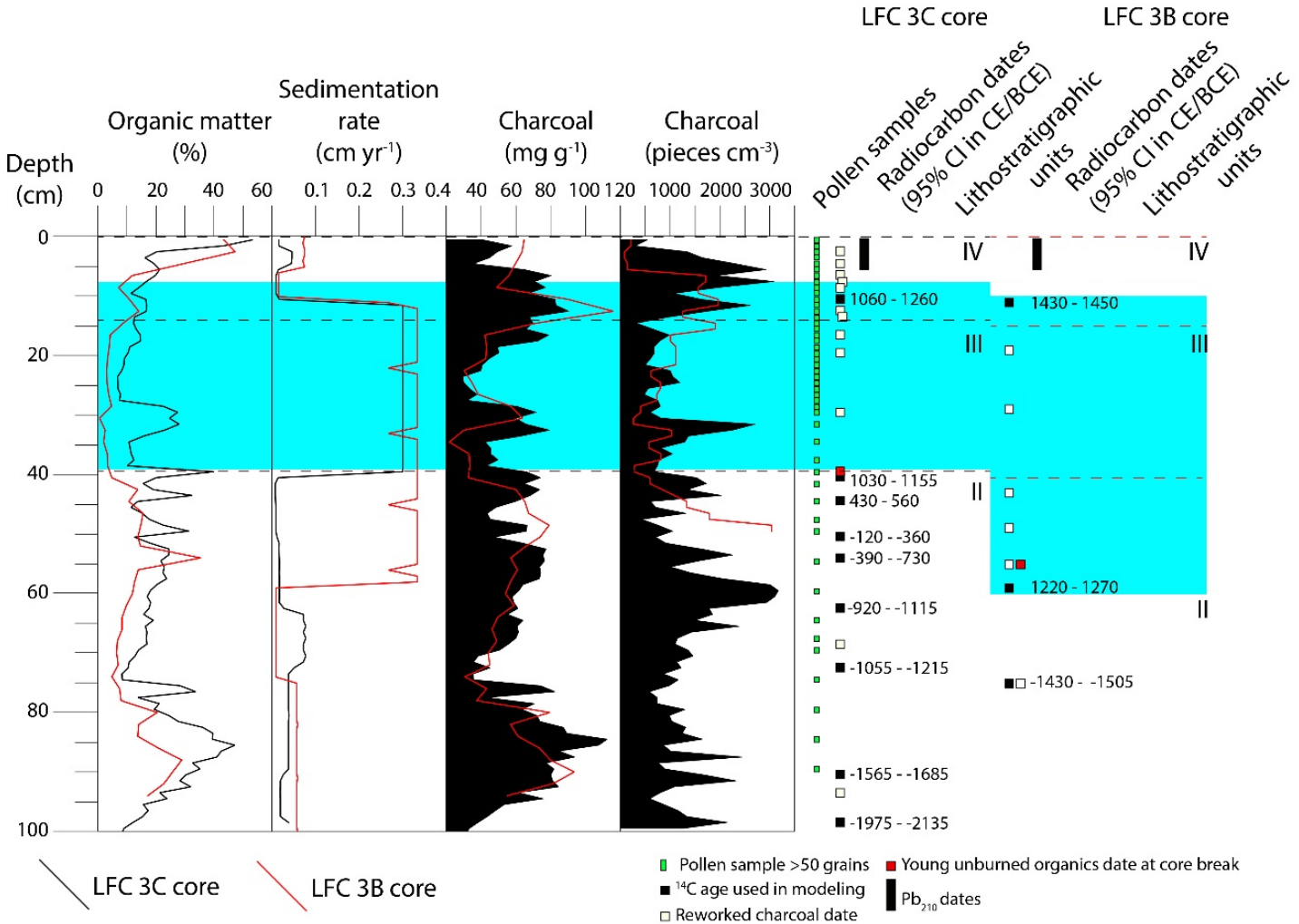

Fig. S18. Stratigraphic plot of organic matter, sedimentation rate, and both chemical digestion (mg g^{-1}) and counted (pieces cm^{-3}) estimates of charcoal concentration for the LFC 3C and 3B cores. Pollen and radiocarbon samples are also indicated. The turquoise zone is the depth range that the age-model includes within the Hemish occupation (ca. 1100-1650 CE).

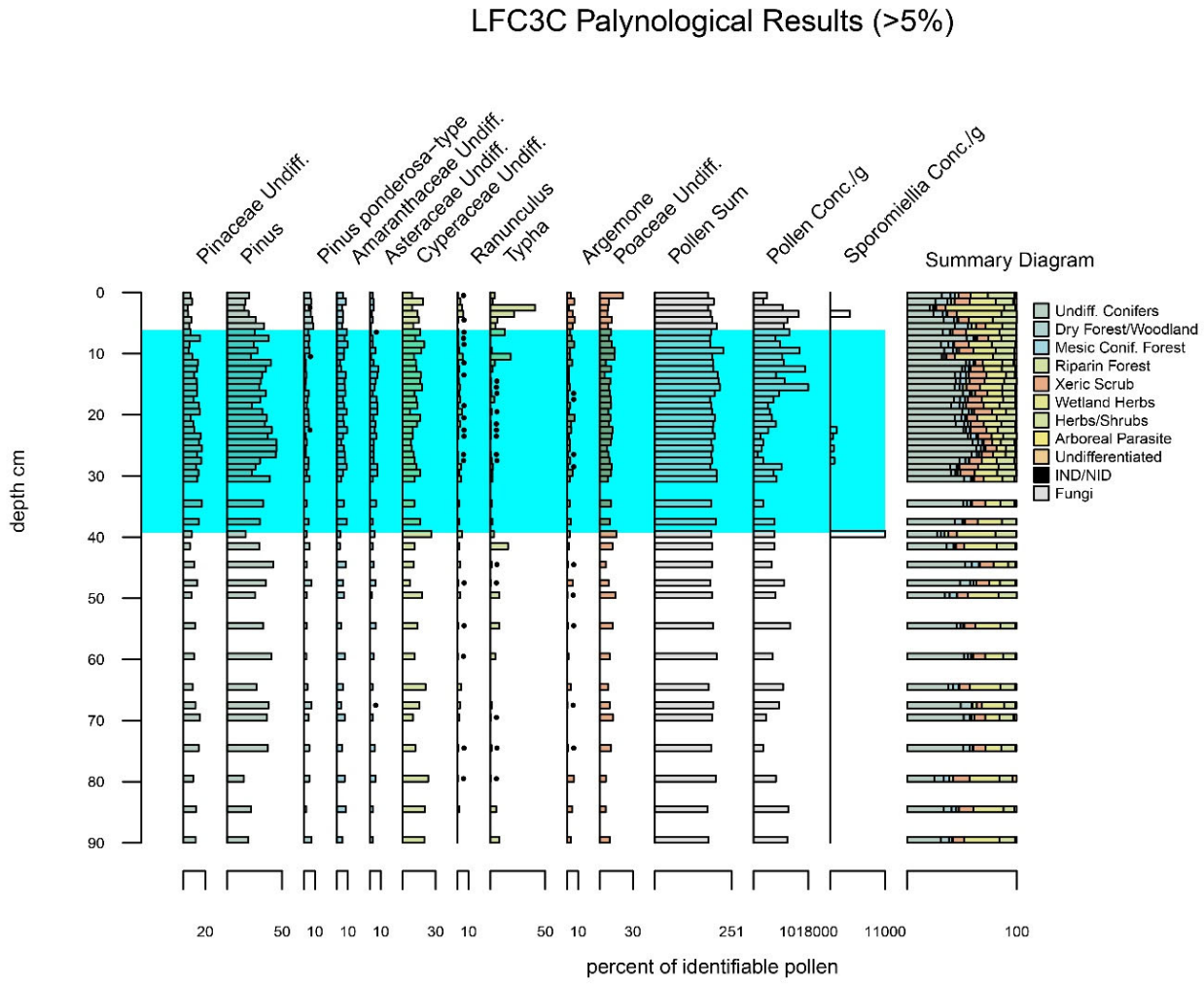

Fig. S19. Stratigraphic plot of pollen percentages for LFC 3C showing only those pollen taxa that reach at least 5% at some point in the profile. The turquoise zone is the depth range that the age-model includes within the Hemish occupation (ca. 1100-1650 CE).

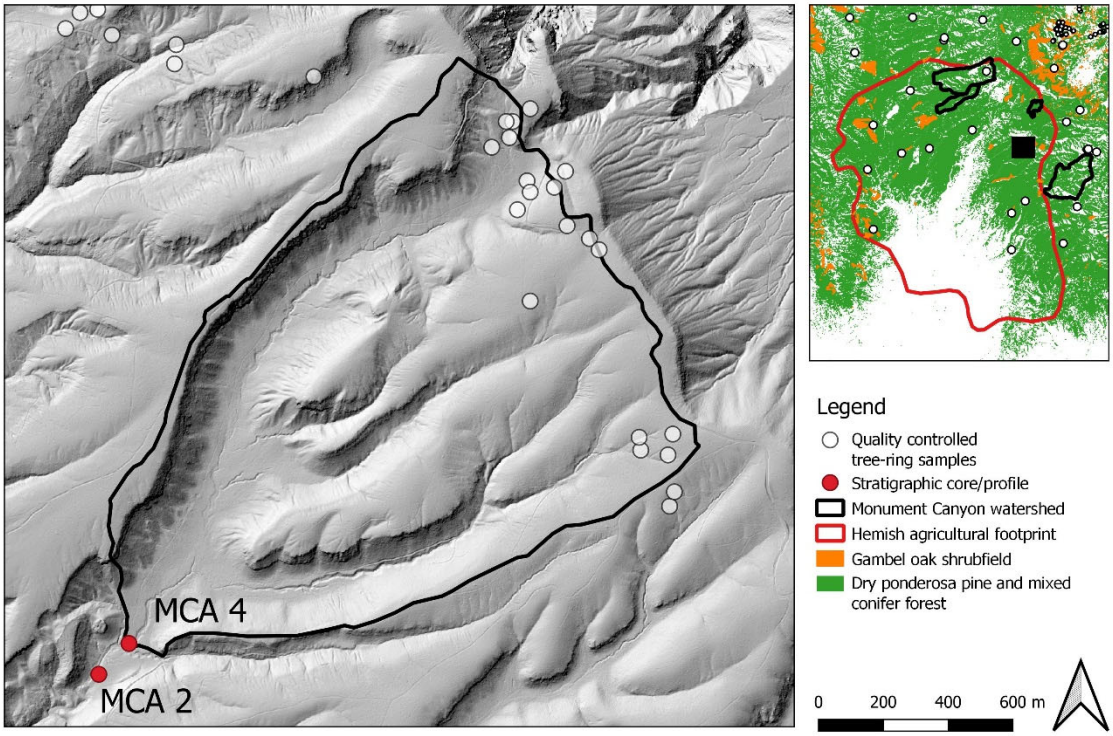

Fig. S20. Topographic map of the watershed catchment for the trench localities below the Monument Canyon Research Natural Area (MCA 4 and MCA 2). Scale apples to primary map tile on the left. Hillshade is from bare-earth LiDAR data provided by the Southwest Jemez Community Forest Landscape Restoration project.

Fig. S21. Landscape context of the trenching location below Monument Canyon Research Natural Area (MCA 4). Figures are working in the trench into a fan terrace that is inset to the major valley fill terrace at the right of the view. View is to the east. (Photo by C. Roos.)

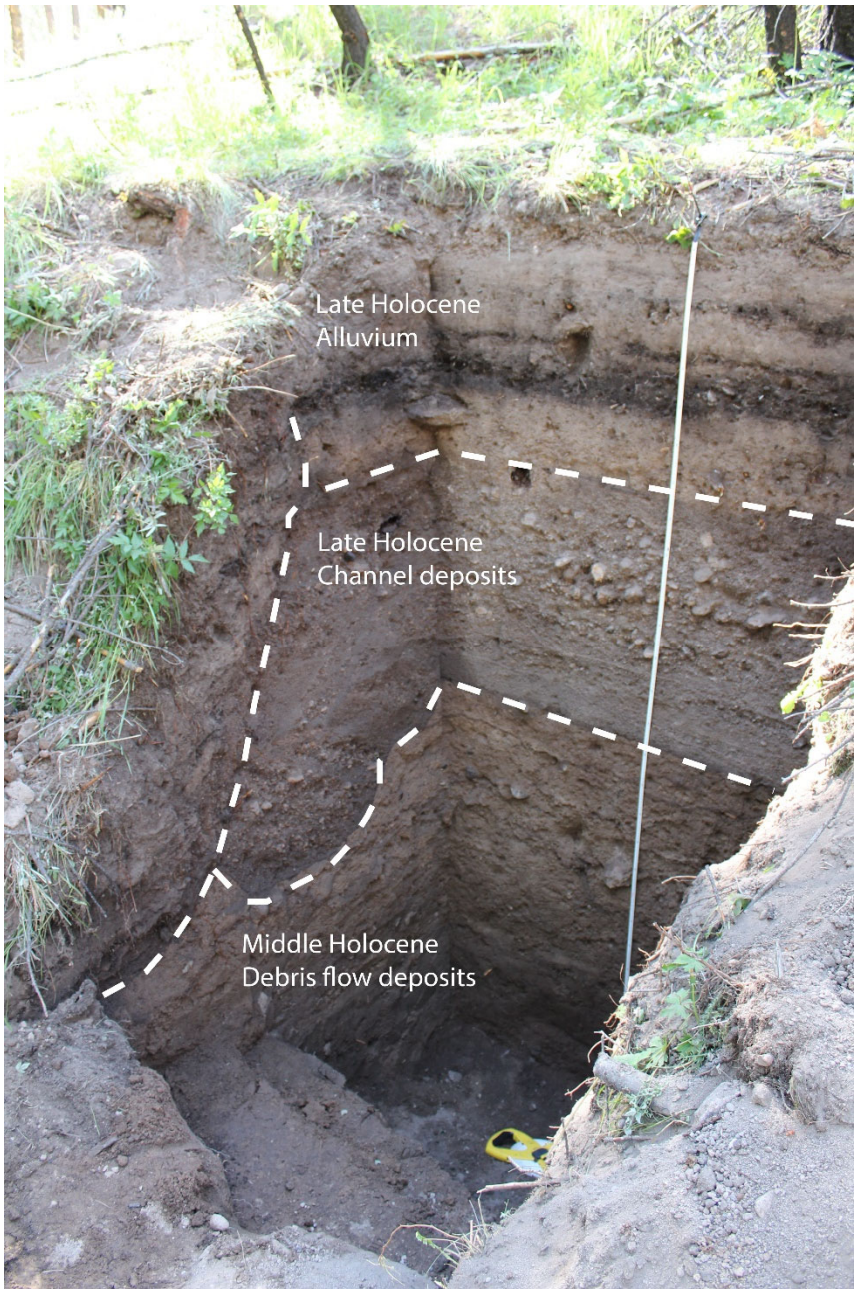

Fig. S22. Stratigraphic photo of MCA 4. Note the paleochannel in center and fine-grained alluvium with dense charcoal layers above this. Strata below the channel are not discussed in this paper. View is to the northeast. (Photo by C. Roos.)

Fig. S23. Stratigraphic photo of MCA 4B column after headcutting and erosion in 2013-2014. Note the paleochannel in center and fine-grained alluvium with dense charcoal layers above this. Strata below the channel are not discussed in this paper. View is to the north/northeast. Original MCA 4 trench is at the right of the exposed profile (Photo by C. Roos.)

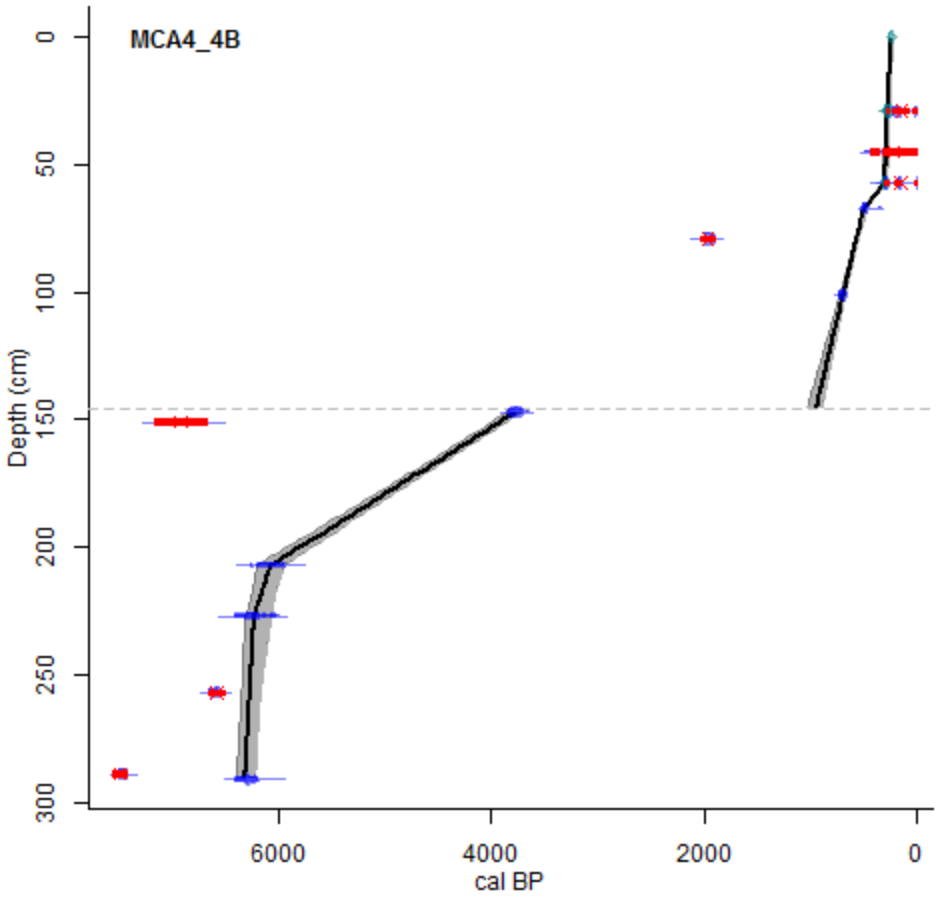

Fig. S24. Age-depth model from for the MCA4 and MCA 4B. Red bars indicate 2σ calibrated age ranges of old or reworked charcoal ages or standard calibrated ages (near top that are superceded by Bayesian calibrations) that were excluded from the model. Blue bars indicate 2σ calibrated age ranges of charcoal dates that were included from the model.

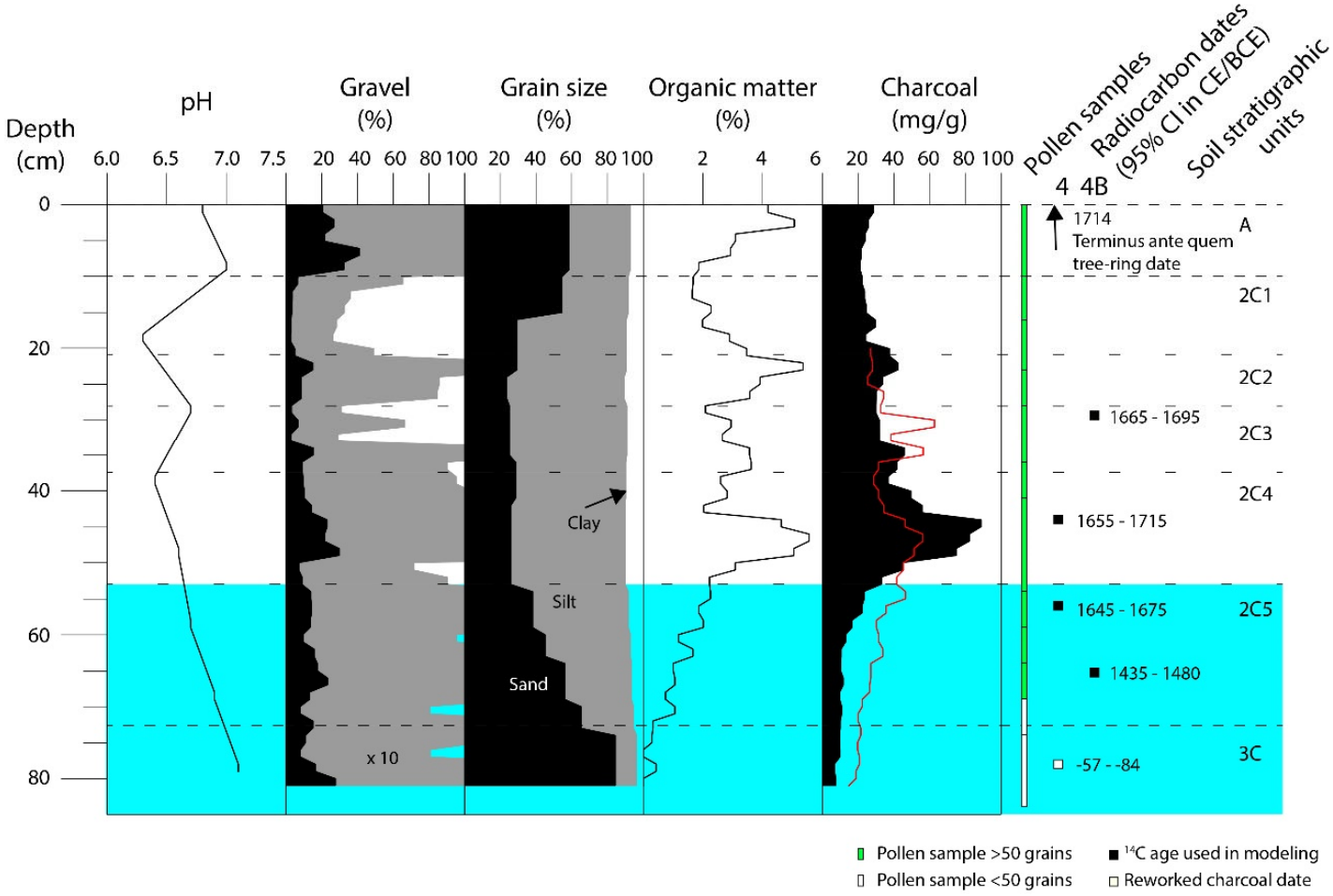

Fig. S25. Stratigraphic plot of pH, gravel, grain size distributions, organic matter, and charcoal concentrations for the upper section of MCA 4 and MCA 4B. Also indicated are the soil horizons and the location of pollen samples and radiocarbon dates used in the age model. The turquoise zone is the depth range that the age-model includes within the Hemish occupation (ca. 1100-1650 CE).

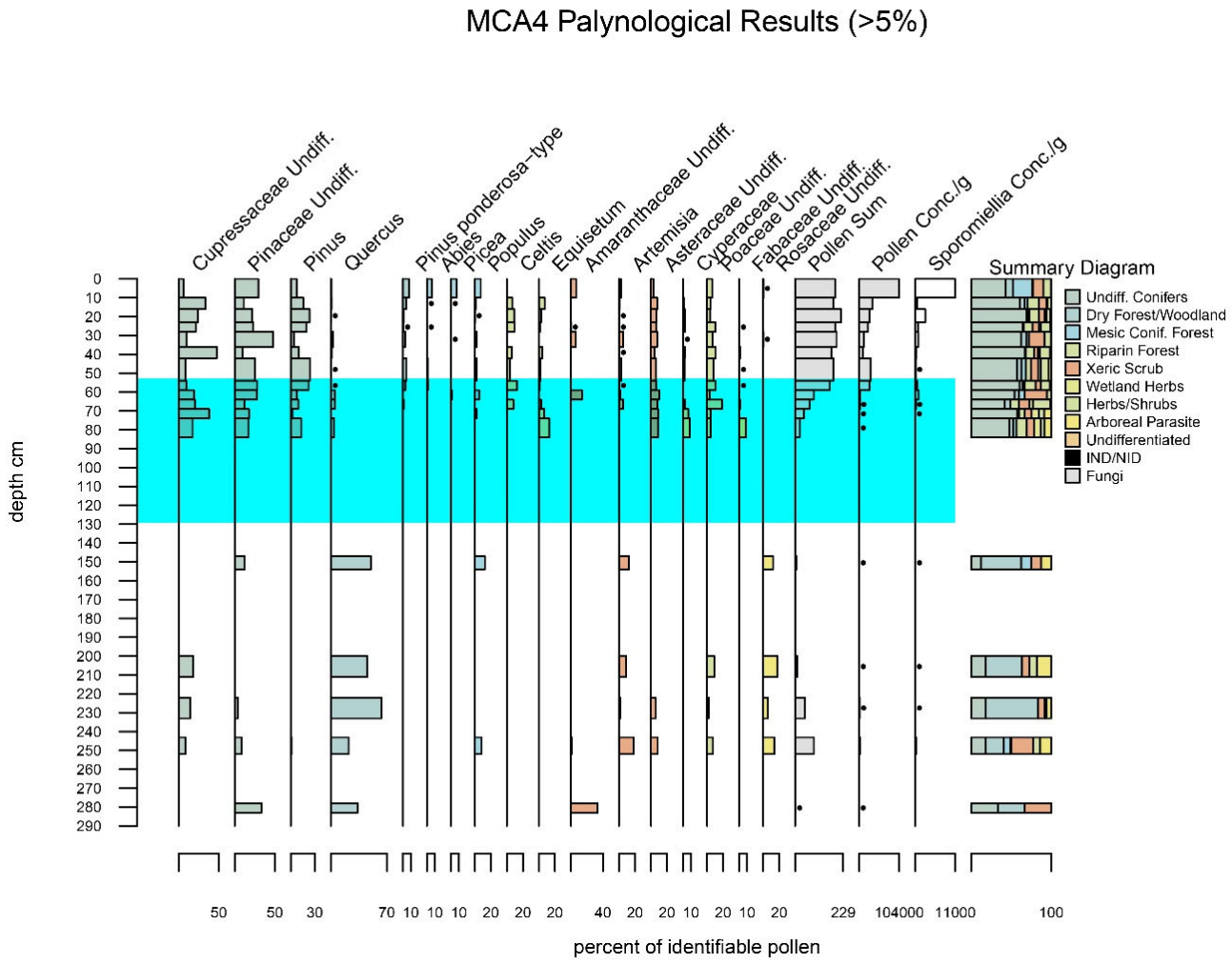

Fig. S26. Stratigraphic plot of pollen percentages for MCA 4 showing only those pollen taxa that reach at least 5% at some point in the profile. The turquoise zone is the depth range that the age-model includes within the Hemish occupation (ca. 1100-1650 CE).

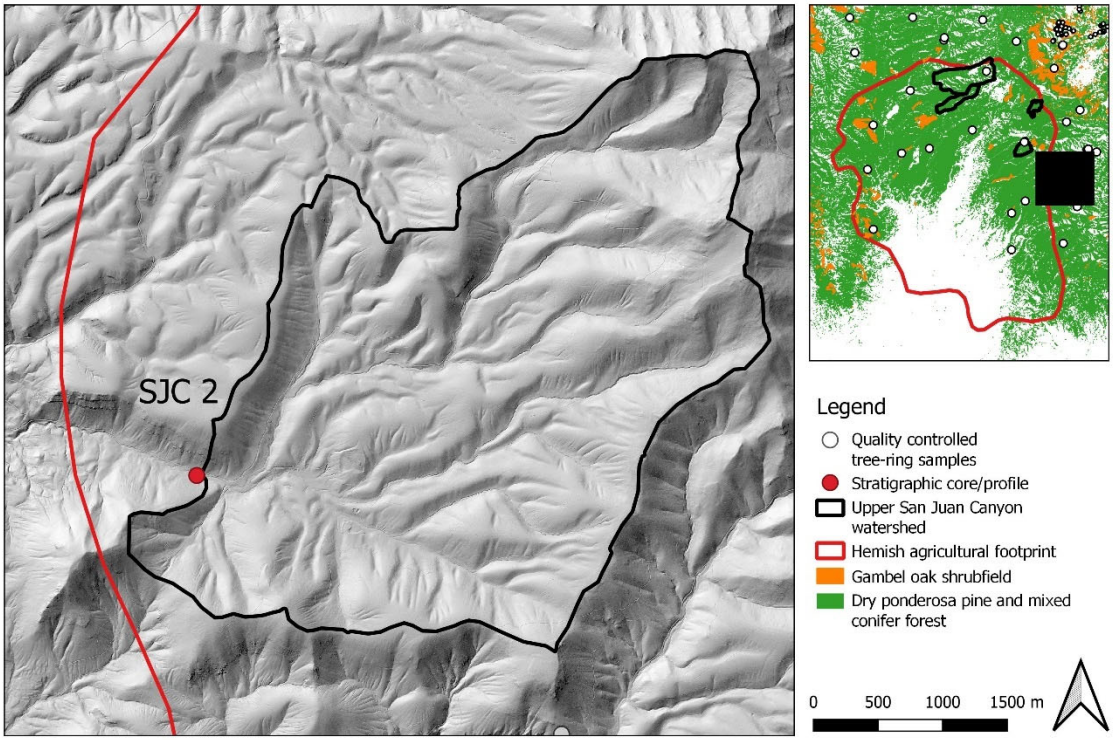

Fig. S27. Topographic map of the watershed catchment for the coring locality in upper San Juan Canyon (SJC 2). Scale apples to primary map tile on the left. Hillshade is from bare-earth LiDAR data provided by the Southwest Jemez Community Forest Landscape Restoration project.

Fig. S28. Landscape context of the coring location in upper San Juan Canyon (SJC 2). The valley fill terrace to the right of the channel (center) is the landform that was cored. View is to the east (upstream). (Photo by C. Roos.)

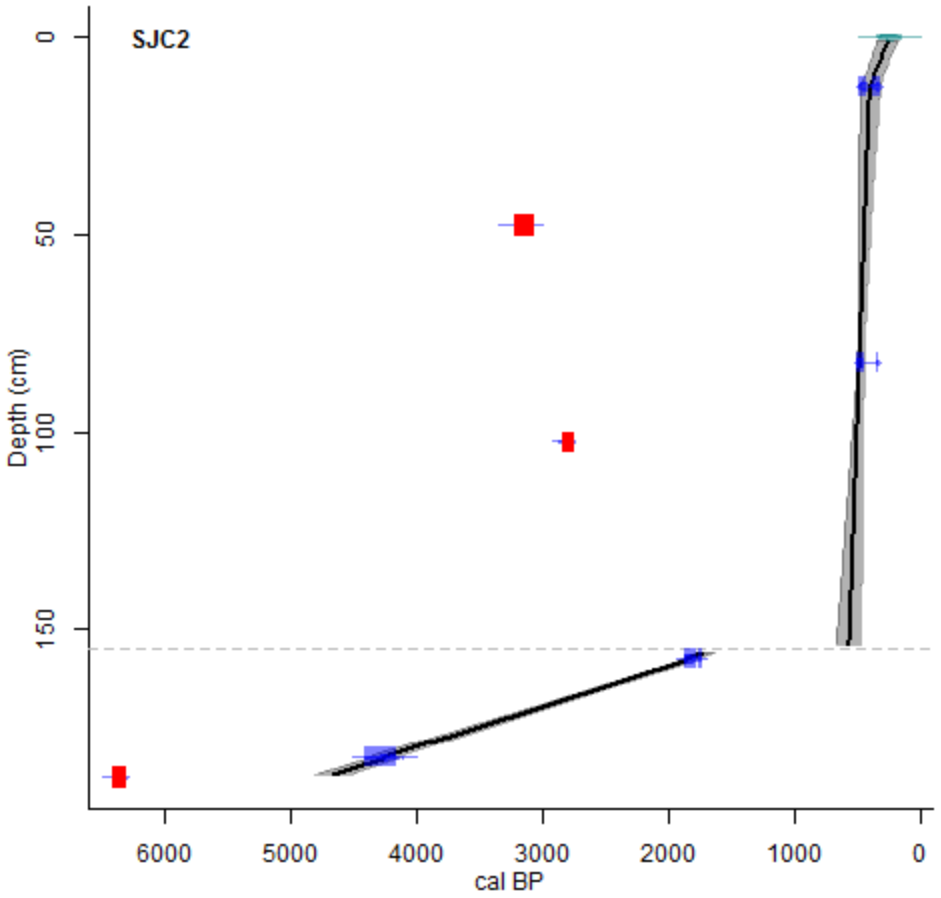

Fig. S29. Age-depth model from for the SJC 2. Red bars indicate 2σ calibrated age ranges of old or reworked charcoal ages that were excluded from the model. Blue bars indicate 2σ calibrated age ranges of charcoal dates that were included from the model.

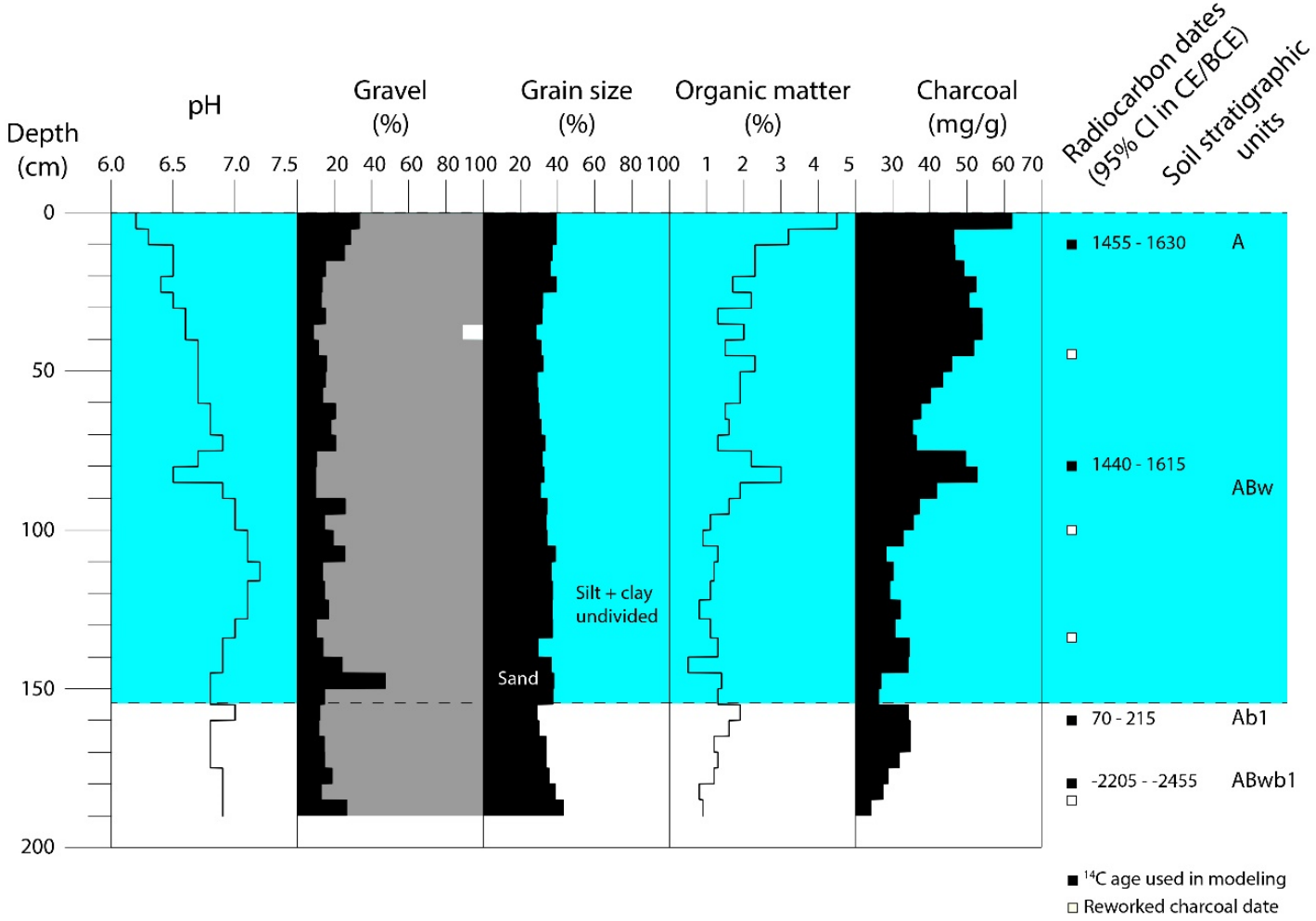

Fig. S30. Stratigraphic plot of pH, gravel, grain size distributions, organic matter, and charcoal concentrations for the SJC 2 core. Also indicated are the soil horizons and the location of radiocarbon dates used in the age model. The turquoise zone is the depth range that the age-model includes within the Hemish occupation (ca. 1100-1650 CE).

Table S1. **Stratigraphic descriptions of the soil and sedimentary units in Banco Bonito 1 cores (BBO 1).**

Depth (cm)	Soil stratigraphic unit	Lithostratigraphic Unit	Description and interpretation
0-5	O	-	Modern surface soil horizon in upward fining (from medium fine subrounded pebbles to medium sand); dark brown (10YR 4/3 (dry), 10YR 3/3 (moist)), loose, single grain with abundant roots. Clear lower boundary. **Decomposing litter layer for the modern soil surface.**
5-55	A1	III	Dark gray to black loam with fine granular structure, very fine roots and a very gradual lower boundary (10YR 4/1 (dry), 10YR 2/1 (moist)). **Uppermost zone of a cumulic soil in mixed colluvial and eolian sediments.**
55-140	A2	III	Dark gray loam with weaker granular structure, fine roots, charcoal, and very gradual lower boundary (10YR 4.5/1 (dry), 10YR 2.5/1 (moist). **Probably a paleosol welded into a cumulic soil in mixed colluvial and eolian sediments.**
140-192	A3	III	Massive, gradually lightening gray loam with distinct lower boundary (10YR 5/2 (dry), 10YR 3/1 (moist). **Probably a paleosol welded into a cumulic soil in mixed colluvial and eolian sediments.**
192-200	Ab1	III	Massive, very dark gray to black loam with diffuse lower boundary (10YR 4/1 (dry), 10YR 2/1 (moist). **Buried soil in mixed colluvial and eolian sediments.**
200-208	ACb1	III	Massive, gray fine sandy loam with a distinct lower boundary (10YR 5/2 (dry), 10YR 3/1 (moist)). **Weathered and organic enriched colluvial and eolian sediments.**
208-236	Ab2	III	Massive, very dark gray very fine sandy loam with distinct lower boundary (10YR 4/2 (dry), 10YR 2/1 (moist)). **Buried soil in mixed colluvial and eolian sediments.**
236-240	Cb2	III	Massive, reddish brown fine sandy loam with a distinct lower boundary (7.5YR 5/2 (dry), 7.5YR 3/4 (moist)). **Mixed colluvial and eolian sediments.**
240-265	Ab3	III	Massive, very dark gray very fine sandy loam that gradually gets lighter with depth with a sharp, wavy lower boundary (10YR 4/2 (dry), 10YR 3/2 (moist)). **Buried soil in mixed colluvial and eolian sediments.**
265-275	ACb3	III	Platy, lighter (10YR 5/3 (dry), 10YR 3/3 (moist)) very fine sandy loam with distinct lower boundary. **Weathering colluvium and eolian sediments.**
275-312	Ab4	III	Massive, charcoal-rich dark gray brown very fine sandy loam with gradual lower boundary (10YR 6/2 (dry), 10YR 3/2 (moist)). **Buried soil formed in colluvial and eolian sediments.**
312-350	Bw1b4	II	Massive, light brownish red sandy loam with rare pebbles and charcoal with a gradual lower boundary (10YR 6/4 (dry), 7.5YR 4/6 (moist)). **Weathered subsoil in colluvium.**
350-418	Bw2b4	II	Massive, reddish brown sandy loam with pebbles and sharp lower boundary (7.5YR 5/4 (dry), 7.5YR 4/6 (moist)). **Weathered subsoil in colluvium.**
418-440	Ab5	II	Massive, gray brown organic rich sandy loam with pebbles and a gradual lower boundary (7.5YR 3/3 (dry), 7.5YR 2.5/3 (moist). **Buried soil formed in colluvium.**

440-500	Bw1b5	II	Massive, reddish brown medium to coarse sandy loam with pebbles and distinct lower boundary (7.5YR 6/4 (dry), 7.5YR 3.5/4 (moist)). **Weathered subsoil in colluvium.**
500-515	Bw2b5	I	Massive, very firm reddish brown silts and clays overlying rhyolite bedrock (7.5YR 6/4 (dry), 7.5YR 3.5/4 (moist)). **Weathered subsoil in eolian sediments.**

Table S2. Radiocarbon data for Banco Bonito 1 cores (BBO 1). Italicized dates were excluded from the age-depth model.

Sample	AMS number	Depth (cm)	Material dated	14C age (mean ± 1 SD)	Calibrated age BP (95% CI)	Calibrated age CE/BCE (95% CI)
BBO 1.5006	Keck-142242	25-30cm	Charcoal: cuticles and bark	795± 25	675-744	1206-1275 CE
BBO 1.5011	Keck-142243	50-55cm	Charcoal, twig	1600 ± 25	1414-1546	404-536 CE
BBO 1.5017	Keck-142244	80-85cm	Charcoal: dense non-wood, and cuticle	1745± 25	1570-1713	237-380 CE
BBO 1.5022	Keck-142245	105-110cm	Charcoal: cuticle and twig	3755± 25	3993-4229	2044-2280 BCE
BBO 1.5027	*Keck-142246*	*130-135cm*	*Charcoal: aggregated cuticle*	*4795± 25*	*5474-5592*	*3525-3643 BCE*
BBO 1.1029	Keck-168898	140-145cm	Charcoal: conifer xylem	4555± 20	5068-5316	3119-3367 BCE
BBO 1.1037	*Keck-168899*	*180-185cm*	*Charcoal: needle*	*6275± 25*	*7166-7257*	*5217-5308 BCE*
BBO 1.1040	*Keck-168900*	*195-200cm*	*Charcoal: conifer xylem*	*6840± 20*	*7617-7697*	*5668-5748 BCE*
BBO 1.1044	Keck-168902	215-220cm	Charcoal: two forb axes, seed, and conifer xylem	5575± 30	6302-6407	4353-4458 BCE
BBO 1.5050	Keck-142247	245-250cm	Charcoal: dense non-conifer	7430± 25	8187-8327	6238-6378 BCE
BBO 1.5059	Keck-142248	290-295cm	Charcoal: glassy char, cuticle, conifer wood fragment	8525± 25	9488-9540	7539-7591 BCE
BBO 1.1081	*Keck-168903*	*400-405cm*	*Bulk soil*	*11645± 50*	*13,374-13,578*	*11,425-11,629 BCE*
BBO 1.1086	Keck-168904	425-430cm	Bulk soil	10470± 45	12,136-12,560	10,187-10,611 BCE
BBO 1.1113	Keck-169580	510-515cm	Bulk soil	21410± 80	25,557-25,912	23,608-23,963 BCE

Table S3. Stratigraphic descriptions of the soil and sedimentary units in Banco Bonito 2 cores (BBO 2).

Depth (cm)	Soil stratigraphic unit	Lithostratigraphic Unit	Description and interpretation
0-30	A	I	Single grain, sandy loam with medium and fine roots and very rare pebbles with a diffuse lower boundary (10YR 3/2 (dry), 10YR 3/1 (moist)). **Soil formed on fine grained alluvial fan deposits.**
30-70	Ab1	I	Upward coarsening from fine to very coarse, single grain sandy loam with medium and fine roots and a diffuse lower boundary (10YR 3/1 (dry), 10YR 3/1 (moist)). **Buried soil formed on fine-grained alluvial fan deposits.**
70-155	Ab2	I	Poorly sorted, single grain sandy loam with subangular very coarse sand and pebbles and a clear lower boundary (10YR 4/1 (dry), 10YR 3/1 (moist)). Lightens in color gradually with depth. **Cumulic buried soil formed on fine-grained alluvial fan deposits.**
155-205	Ab3	I	Single grain, fine sandy loam (10YR 4/2 (dry), 10YR 4/1.5 (moist)). Lightens in color gradually with depth. **Cumulic buried soil formed on fine-grained alluvial fan deposits.**
205-230	Cb3	I	Single grain, medium to coarse loamy sand with pebbles and medium to coarse sand sized charcoal, and diffuse and irregular lower boundary (10YR 5/3 (dry), 10YR 4/2 (moist)). **Unweathered alluvial fan deposits.**
230-275	Ab4	I	Upward fining from medium to fine single grain, sandy loam with common charcoal, a clear lower boundary, and gets lighter in color with depth (10YR 5/2 (dry), 10YR 4/2 (moist)). **Buried soil formed on fine-grained alluvial fan deposits.**
275-397	Ab5	I	Upward fining from coarse to fine single grain, sandy loam with occasional coarse pebbles and rare charcoal, lightens in color with depth, and a distinct lower boundary (10YR 4/2 (dry), 10YR 3/2 (moist). **Cumulic buried soil formed on fine-grained alluvial fan deposits.**
397-477	Ab6	I	Friable, weakly granular loam with common sand sized charcoal pieces, traces of medium sized root casts, and clear lower boundary (10YR 5/3 (dry), and 10YR 4/2 (moist)). **Cumulic buried soil formed on fine-grained alluvial fan deposits.**
477-560	Cb6	I	Single grain, medium to coarse sands with interbedded silt laminae between 2-10cm thick. **Unweathered alluvial fan deposits.**

Table S4. Radiocarbon data for Banco Bonito 2 cores (BBO 2). Italicized dates were excluded from the age-depth model.

Sample	AMS number	Depth (cm)	Material dated	14C age (mean ± 1 SD)	Calibrated age BP (95% CI)	Calibrated age CE/BCE (95% CI)
BBO 2.4004	Keck-161805	15-20cm	Charcoal: cuticle, bark scale, seed shells	225 ± 20	1-305	1645-1949 CE
BBO 2.1007	Keck-168906	30-35cm	Charcoal: angiosperm wood and cuticle	590 ± 15	544-641	1309-1406 CE
BBO 2.4008	*Keck-161806*	*35-40cm*	*Charcoal: cuticle and glassy carbon*	*930 ± 20*	*794-914*	*1036-1156 CE*
BBO 2.4012	Keck-163083	55-60cm	Charcoal: cuticle, needle	855 ± 15	732-788	1162-1218 CE
BBO 2.4016	Keck-161807	75-80cm	Charcoal: cuticle and needle fragment	1290 ± 20	1182-1282	668-768 CE
BBO 2.4025	Keck-161808	120-125cm	Charcoal: cuticle and glassy carbon	1935 ± 20	1826-1927	23-124 CE
BBO 2.4033	Keck-161809	160-165cm	Charcoal: cuticle	2410 ± 20	2353-2675	404-726 BCE
BBO 2.4043	Keck-161810	210-215cm	Charcoal: cuticle	2575 ± 20	2717-2751	768-802 BCE
BBO 2.4048	Keck-163084	235-240cm	Charcoal: cuticle, twig	2650 ± 15	2748-2776	799-827 BCE
BBO 2.1055	Keck-142249	270-275cm	Charcoal: cone scale	3280 ± 25	3453-3565	1504-1616 BCE
BBO 2.4059	Keck-163085	285-290cm	Charcoal: cuticle, unidentified wood	3440 ± 15	3639-3817	1690-1868 BCE
BBO 2.1070	Keck-142250	340-345cm	Charcoal: conifer twig	4540 ± 25	5054-5313	3105-3364 BCE
BBO 2.4083	Keck-163086	402-407cm	Charcoal: cuticle, axis	5155 ± 20	5896-5983	3947-4034 BCE
BBO 2.1112	Keck-142251	545-550cm	Charcoal: conifer xylem	5775 ± 25	6497-6654	4548-4696 BCE

Table S5. Stratigraphic descriptions of the soil and sedimentary units in Cebollita Springs 3 cores (CBS 3).

Depth (cm)	Soil stratigraphic unit	Lithostratigraphic Unit	Description and interpretation
0-35	A	XI	Modern surface soil horizon in dark gray brown to gray fine subangular blocky to coarse granular silt loams (10YR 5/1 (dry), 10YR 2/2 (moist)), with common coarse charcoal and 4-8mm orange iron oxyhydroxide mottles. Distinct lower contact **Soil formed on fine grained slopewash and eolian deposits.**
35-58	2C	X	Poorly sorted angular to subangular gravels with interstitial and interbedded (46-49cm) gray to very dark gray (10YR 6/1 (dry), 10YR 3/1 (moist)) sandy loams. **Colluvial deposits with eolian and paludal contributions.**
58-80	3Ab1	IX	Gray to black (10YR 5/1 (dry), 10YR 2.5/2 (moist)), massive silt loam with common flecks of fine charcoal. Few fine roots and rare fine charcoal. Diffuse lower boundary. **Soil formed on fine grained slopewash and eolian deposits.**
80-110	4Cb1	IIX	Very poorly sorted subangular to angular pebbles and dark gray muds (10YR 6/1 (dry), 10YR 3/2 (moist)) Diffuse lower boundary. **Colluvial deposits with eolian and paludal contributions.**
110-140	5Ab2	VII	Upward fining very dark gray to black massive muds (10YR 1.5/1 (moist)), Diffuse lower boundary. **Soil formed on fine grained slopewash and eolian deposits.**
140-160	6Cb2	VI	Slightly upward fining moderately well sorted gravels to very coarse sands. Clear lower boundary. **Colluvial deposits with slopewash, eolian and paludal contributions.**
160-222	7Ab3	V	Very poorly sorted dark gray massive, muds (10YR 3.2 (moist)) with abundant gravel and very coarse sand. Very abrupt, smooth lower boundary. **Soil formed in colluvial deposits with slopewash, eolian and paludal contributions.**
222-228	8Ab4	IV	Well sorted dark gray to black, massive muds (10YR 3.2 (moist)). **Soil formed on fine grained slopewash, paludal and eolian deposits.**
228-258	9Cb4	III	Alternating beds of moderately well sorted to very well sorted very coarse sands and gravels.
258-265	10A1b5	II	Very dark gray, poorly sorted, single grain silts and sands. **Soil formed on fine grained slopewash, paludal and eolian deposits.**
265-310	11A2b5	I	Upward fining from coarse sands with subangular pebbles to sandy loams with subangular pebbles. **Soil formed in colluvial deposits with slopewash, eolian and paludal contributions.**

Table S6. Radiocarbon data for Cebollita Springs 3 cores (CBS 3). Italicized dates were excluded from the age-depth model.

Sample	AMS number	Depth (cm)	Material dated	14C age (mean ± 1 SD)	Calibrated age BP (95% CI)	Calibrated age CE/BCE (95% CI)
CBS 3.203	*Keck-168907*	*10-15cm*	*Charcoal: cone scales (2) and seed*	*1000 ± 20*	*805-961*	*989-1145 CE*
CBS 3.104	*Keck-161811*	*15-20cm*	*Charcoal: cuticle and twig fragments*	*755 ± 20*	*668-725*	*1225-1282 CE*
CBS 3.206	Keck-151920	25-30cm	Charcoal: fecal pellet?	690 ± 20	568-678	1272-1382 CE
CBS 3.212	Keck-151921	55-60cm	Charcoal: seed	665 ± 20	563-670	1280-1387 CE
CBS 3.213	*Keck-151922*	*60-65cm*	*Unidentified non-conifer charcoal*	*1220 ± 20*	*1067-1234*	*716-883 CE*
CBS 3.113	*Keck-163079*	*60-65cm*	*Charcoal: cuticle, needle bundle base*	*900 ± 15*	*748-906*	*1044-1202 CE*
CBS 3.115	Keck-161812	70-75cm	Charcoal: cuticle and needle fragment	785 ± 20	679-730	1220-1271 CE
CBS 3.222	*Keck-151923*	*105-110cm*	*Charcoal: fecal pellet?*	*3660 ± 20*	*3906-4082*	*1957-2133 BCE*
CBS 3.124	Keck-163080	115-120cm	Charcoal: cuticle, xylem	2410 ± 15	2356-2485	407-536 BCE
CBS 3.126	Keck-161813	125-130cm	Charcoal cuticle, axis, and needle fragment	2675 ± 20	2750-2843	801-894 BCE
CBS 3.234	Keck-151924	165-170cm	Charcoal: conifer xylem	3845 ± 20	4155-4403	2206-2454 BCE
CBS 3.240	Keck-168908	195-200cm	Charcoal: conifer and angiosperm xylem	3890 ± 15	4252-4412	2303-2463 BCE
CBS 3.144	Keck-161814	215-220cm	Charcoal: wood	4210 ± 20	4652-4842	2703-2893 BCE
CBS 3.253	Keck-168909	260-265cm	Charcoal: cuticle and conifer xylem	4355 ± 20	4859-4968	2910-3019 BCE
CBS 3.155	Keck-161815	270-275cm	Charcoal: cuticle and conifer xylem	4645 ± 25	5311-5463	3362-3514 BCE

Table S7. Stratigraphic descriptions of sedimentary units Lake Fork Canyon 3 cores (LFC 3B and 3C).

Depth 3B (cm)	Depth 3C (cm)	Lithostratigraphic Unit	Description and interpretation
0-12	0-14	IV	Predominantly organic (histic) dark reddish gray to black mucks. **Slow organic sedimentation with eolian input.**
12-41	14-39	III	Predominantly inorganic gray brown to dark gray massive silts and clays grading upward to finely laminated silts and very fine sand in LFC 3B and interbedded peat ~30 cm within massive very dark gray clays in LFC 3C. **Rapidly accumulating terrigenous sediments (eolian and slopewash).**
41-117	39-102	II	Massive, very dark reddish brown peats and muds interbedded with ~10 cm thick lenses of dark gray clays and charcoal at ~70 cm and 100 cm in LFC 3C. Very dark gray brown organic silty muds with charcoal at LFC 3B. **Slow organic and terrigenous sedimentation.**
117-137	-	I	Massive, gray very fine sands and silts with fine roots and traces of fine charcoal. **Incipient soil on terrigenous sediments.**

Table S8. Pb-210 and Cs-137 concentrations (disintegrations per minute) and age estimates for the Lake Fork Canyon cores (LFC 3B and LFC 3C). Italicized dates were excluded from the age-depth model.

Sample	Lab no.	Depth (cm)	Pb-210 (total) (dpm/g)	Pb-210 (excess) (dpm/g)	Cs-137 (dpm/g)	Constant Initial Concentration (CIC) model age estimates (CE)
LFC 3b.01	*EC-1022*	*0-2cm*	*14.81 ± 0.71*	*11.30 ± 0.75*	*0.99*	-
LFC 3b.02	*EC-1023*	*2-4cm*	*16.12 ± 0.91*	*13.33 ± 0.96*	*0.77*	-
LFC 3b.03	*EC-1024*	*4-6cm*	*8.57 ± 0.48*	*4.80 ± 0.52*	*0.78*	*1900 ± 50*
LFC3c.001	*EC-1025*	*0-1cm*	*11.70 ± 0.54*	*7.59 ± 0.58*	*1.70*	*2008 ± 4*
LFC-3c.002	*EC-1026*	*1-2cm*	*9.41 ± 0.51*	*4.21 ± 0.57*	*0.63*	*2000 ± 4*
LFC3c.003	*EC-1027*	*2-3cm*	*10.27 ± 0.51*	*3.56 ± 0.58*	*0.00*	*1984 ± 12*
LFC-3c.004	*EC-1028*	*3-4cm*	*6.71 ± 0.39*	*0.51 ± 0.45*	*0.00*	*1967 ± 5*
LFC3c.005	*EC-1029*	*4-5cm*	*5.64 ± 0.44*	*1.70 ± 0.49*	*0.00*	*1912 ± 50*
LFC-3c.006	EC-1030	5-6cm	3.74 ± 0.30	0.10 ± 0.35	0.00	1812 ± 50

Table S9. Radiocarbon data for Lake Fork Canyon bog core 3B (LFC 3B). Italicized dates were excluded from the age-depth model.

Sample	AMS number	Depth (cm)	Material dated	14C age (mean ± 1 SD)	Calibrated age BP (95% CI)	Calibrated age CE/BCE (95% CI)
LFC 3B.6	Keck-172529	10-12cm	Bulk sediment <250 microns	450 ± 15	498-520	1430-1452 CE
LFC 3B.10	*Keck-172530*	*18-20cm*	*Bulk sediment <250 microns*	*1185 ± 15*	*1065-1174*	*776-885 CE*
LFC 3B.15	*Keck-163072*	*28-30cm*	*Charcoal: cuticle*	*1840 ± 35*	*1701-1871*	*79-249 CE*
LFC 3B.22	*Keck-163073*	*42-44cm*	*Charcoal: cuticle, needle frag, seed*	*2050 ± 15*	*1949-2101*	*1 CE - 152 BCE*
LFC 3B.25	*Keck-151928*	*48-50cm*	*Charcoal: conifer (outer ring)*	*2515 ± 20*	*2496-2735*	*547-786 BCE*
LFC 3B.28	*Keck-165067*	*54-56cm*	*Charcoal: cuticle*	*1585 ± 45*	*1377-1563*	*387-573 CE*
LFC 3B.28	*Keck-172531*	*54-56cm*	*Bulk sediment <250 microns*	*385 ± 20*		
LFC 3B.30	Keck-151929	58-60cm	Unburned sedge	785 ± 20	679-730	1220-1271 CE
LFC 3B.38	Keck-151930	74-76cm	Charcoal: conifer wood	2990 ± 20	3077-3228	1128-1279 BCE
LFC 3B.47	Keck-165047	92-94cm	Charcoal: cuticle and uncharred cuticle	3205 ± 20	3381-3455	1432-1506 BCE
LFC 3B.54	Keck-163076	106-108cm	Charcoal: axis and needle frag	3720 ± 20	3985-4146	2036-2197 BCE
LFC 3B.65	Keck-163077	128-130cm	Charcoal: cuticle, axis, needle, seed, UNWC	4740 ± 35	5327-5585	3378-3636 BCE

Table S10. Radiocarbon data for Lake Fork Canyon bog core 3C (LFC 3C). Italicized dates were excluded from the age-depth model.

Sample	AMS number	Depth (cm)	Material dated	14C age (mean ± 1 SD)	Calibrated age BP (95% CI)	Calibrated age CE/BCE (95% CI)
LFC 3C.3	*Keck-165066*	*3cm*	*Charred fecal pellet*	*740 ± 20*	*663-695*	*1255-1287 CE*
LFC 3C.5	*Keck-165065*	*5cm*	*Three charred axes*	*840 ± 30*	*686-891*	*1059-1264 CE*
LFC 3C.7	*Keck-163078*	*7cm*	*Aggregated microcharcoal (cuticle and seed)*	*1020 ± 15*	*924-959*	*991-1026 CE*
LFC 3C.8	*Keck-165069*	*8cm*	*Misc. charred stems and cuticles + misc. charcoal (added 10/28)*	*1840 ± 30*	*1708-1864*	*86-242 CE*
LFC 3C.9	*Keck-187535*	*9cm*	*Bulk sediment <250 microns*	*1025 ± 15*	*926-960*	*989-1023 CE*
LFC 3C.11	Keck-165070	11cm	Charred axis and cuticle + misc. charcoal	845 ± 30	689-892	1058-1261 CE
LFC 3C 13	*Keck-187536*	*13cm*	*Bulk sediment <250 microns*	*1010 ± 15*	*921-956*	*993-1028 CE*
LFC 3C.14	*Keck-165063*	*14cm*	*Charred axis (one piece)*	*1615 ± 40*	*1407-1602*	*348-543 CE*
LFC 3C.17	*Keck-165062*	*17cm*	*Charred cuticle (one piece)*	*1330 ± 30*	*1184-1301*	*649-766 CE*
LFC 3C.20	*Keck-165061*	*20cm*	*Charred cone scale*	*1900 ± 15*	*1820-1881*	*69-130 CE*
LFC 3C.30	*Keck-172532*	*30cm*	*Bulk sediment <250 microns*	*1810 ± 15*	*1707-1814*	*136-243 CE*
LFC 3C.40	*Keck-187537*	*40cm*	*Bulk sediment <250 microns*	*205 ± 25*	*-4-297*	*1653-1954 CE*
LFC 3C.41	Keck-168910	41cm	Charred seed	935 ± 25	793-919	1031-1157 CE
LFC 3C.45	Keck-172533	45cm	Bulk sediment <250 microns	1545 ± 15	1387-1522	428-563 CE
LFC 3C.51	Keck-168911	51cm	Misc. charred needles	2170 ± 30	2066-2309	117-360 BCE
LFC 3C.55	Keck-168912	54-55cm	Misc. charred needles and cuticle	2380 ± 35	2340-2678	391-729 BCE
LFC 3C.63	Keck-168913	63cm	charred pinus needles and xylem	2850 ± 35	2868-3065	919-1116 BCE
LFC 3C.14C.1	*Keck-152111*	*69cm*	*charred pinus needles*	*3220 ± 60*	*3270-3585*	*1321-1636 BCE*
LFC 3C.73	Keck-168914	73cm	charred pinus needle bundle	2940 ± 20	3005-3164	1056-1215 BCE
LFC 3C.91	Keck-172534	91cm	Bulk sediment <250 microns	3340 ± 15	3513-3633	1563-1683 BCE
LFC 3C.94	*Keck-168915*	*94cm*	*Charred twig*	*3710 ± 55*	*3897-4231*	*1948-2282 BCE*
LFC 3C.14C.3	Keck-151931	98-99	charred pinus needle bundle	3670 ± 20	3926-4084	1977-2001 BCE

Table S11. Stratigraphic descriptions of the soil and sedimentary units in the upper, late Holocene section of Monument Canyon 4 (MCA 4).

Depth (cm)	Soil stratigraphic unit	Lithostratigraphic Unit	Description and interpretation
0-10	A	IV	Modern surface soil horizon in upward fining (from medium fine subrounded pebbles to medium sand); dark brown (10YR 4/3 (dry), 10YR 3/3 (moist)), loose, single grain with abundant roots. Clear lower boundary. **Soil formed on alluvial channel fan.**
10-23	2C1	IV	Massive loamy sands with hints of sub-parallel bedding that decreases upward. Dark punctuations of charcoal or organic matter within a very dark gray (7.5YR 4/1 (dry), 7.5YR 3/1 (moist)) matrix. Few roots. Clear/abrupt lower boundary. **Lateral alluvial channel fan deposits with weak pedogenic alteration.**
23-28	2C2	IV	Dark brown to black (7.5YR 3/2 (dry), 7.5YR 2.5/1 (moist)) bioturbated, single grain very fine sandy loam with abundant very course sand to pebble sized fragments of charcoal. Few fine roots and rare, fine subrounded pebbles. Lower boundary is gradual to distinct. **Post-fire overbank alluvial deposit.**
28-36	2C3	IV	Brown (7.5YR 5/2 (dry), 7.5YR 4/2 (moist)), massive, very fine sandy loam. Few fine roots and rare fine charcoal. Clear to abrupt lower boundary. **Overbank alluvial deposit**.
36-54	2C4	IV	Vert dark gray to black (7.5YR 3/1 (dry), 7.5YR 2.5/1 (moist)), single grain gravelly fine sandy loam with some upward fining and interbedded very fine sand. Very abundant fine roots and abundant subrounded pebbles (mostly pumice). Clear to abrupt lower boundary. **Post-fire overbank alluvial deposit.**
54-74	2C5	IV	Dark brown to brown (7.5YR 5/2 (dry), 7.5YR 3/3 (moist)), massive loamy sands with uncommon, subrounded tuff pebbles and one tuff cobble. Few fine roots and hints of preserved horizontal bedding. Very abrupt, smooth lower boundary. **Alluvial channel fan deposits.**
74-84	3C1	III	Dark brown to brown (10YR 4/3 (dry), 10YR 3/3 (moist)) single grain upward fining set of medium sand and few subrounded pebbles. Capped with a discontinuous 0.5cm thick lens of fine charcoal. **Alluvial channel deposit.**
84-126	3C2	III	Light brownish gray to brown (10YR 6/2 (dry), 10YR 4/2 (moist)) single grain very gravelly coarse sand. Sub-horizontal beds with imbricated, subrounded cobbles of both tuff and pumice. Very abrupt, smooth lower boundary. **Alluvial channel deposit.**
126-147	3C3	III	Dark grayish brown to brown (10YR 4/3 (dry), 10YR 4/2 (moist)) horizontal to cross-bedded medium and coarse sands that is laterally traceable to the base of a paleochannel with a very abrupt lower boundary. **Alluvial channel deposits.**

Table S12. Radiocarbon data for Monument Canyon stratigraphic sections 4 and 4B (MCA 4 and MCA 4B). Italicized dates were excluded from the age-depth model.

Sample	AMS number	Depth (cm) (adjusted depth for 4B)	Material dated	14C age (mean ± 1 SD)	Calibrated age BP (95% CI)	Calibrated age BP (95% CI)	Bayesian calibrated age BP (95% CI)*
MCA 4B.05	Keck-151913	28-30cm	Charcoal: pinus needle base	160 ± 20	1-283	1667-1949 CE	1667-1697 CE
MCA 4.023	*AA102980*	*44-46cm*	*Unidentified charcoal*	*198 ± 74*	*1-429*	*1521-1949 CE*	*1657-1713 CE*
MCA 4.029	Keck-142252	56-48cm	Charcoal: two pine needle fragments	225 ± 25	1-308	1642-1949 CE	1643-1675 CE
MCA 4B.24	Keck-151914	66-68cm	Charcoal: cone scale	425 ± 20	469-516	1434-1481 CE	-
MCA 4.040	*Keck-142253*	*78-80cm*	*Charcoal: cuticle, seeds, glassy char*	*2010 ± 25*	*1893-2033*	*57 CE - 84 BCE*	-
MCA 4B.41	Keck-151915	100-102cm	Unidentified non-conifer charcoal	760 ± 20	670-726	1224-1280 CE	-
MCA 4.074	Keck-142254	146-148cm	Bulk sediment	3495 ± 25	3696-3838	1747-1849 BCE	-
MCA 4.076	*AA102981*	*150-152cm*	*Unidentified charcoal*	*6029 ± 75*	*6676-7155*	*4727-5206 BCE*	-
MCA 4.104	AA102982	206-208cm	Unidentified charcoal	5299 ± 64	5930-6268	3981-4319 BCE	-
MCA 4.114	AA102983	226-228cm	Unidentified charcoal	5459 ± 72	6016-6404	4067-4131 BCE	-
MCA 4.129	Keck-142255	256-258cm	Bulk sediment	5790 ± 25	6505-6659	4556-4710 BCE	-
MCA 4.145	*Keck-142256*	*288-290cm*	*Bulk sediment*	*6580 ± 30*	*7429-7560*	*5480-5611 BCE*	-
MCA 4.147	AA102984	292-294cm	Unidentified charcoal	5484 ± 58	6183-6405	4234-4456 BCE	-

***** Bayesian calibration used the stratigraphic positioning of the three dates and the 1714 CE terminus ante quem age for the surface of the fan to constrain the posterior probabilities of the calibrated ages using BCal (10).

Table S13. Stratigraphic descriptions of the soil and sedimentary units in Upper San Juan Canyon 2 cores (SJC 2).

Depth (cm)	Soil stratigraphic unit	Lithostratigraphic Unit	Description and interpretation
0-95	A	I	Modern surface soil horizon in very dark grayish brown (10YR 4/2 (dry), 10YR 2/2 (moist)), loams with traces of pumice pebbles increasing towards the top. Displays weak, friable subangular blocky structure (moderately expressed below 50cm). Fine roots are common. Gradual lower boundary. **Cumulic soil formed in alluvial deposits.**
95-150	ABw	I	Massive to very weakly granular dark brown to brown (7.5YR 5/3 (dry), 7.5YR 3/3 (moist)) loams with rare tuff and pumice pebbles. Clear/abrupt lower boundary. **Cumulic soil formed in alluvial deposits.**
150-175	Ab1	I	Dark brown to brown (7.5YR 4/2 (dry), 7.5YR 3/2 (moist)) loams with moderate subangular blocky to coarse granular structure. Lower boundary is gradual to distinct. **Soil formed in alluvial deposits.**
175-190	ABwb1	I	As above but grades to coarser subangular blocky structure. **Soil formed in alluvial deposits.**

Table S14. Radiocarbon data for Upper San Juan Canyon stratigraphic section 2 (SJC 2). Italicized dates were excluded from the age-depth model.

Sample	AMS number	Depth (cm)	Material dated	14C age (mean ± 1 SD)	Calibrated age BP (95% CI)	Calibrated age CE/BCE (95% CI)
SJC 2.203	Keck-161817	10-15cm	Charred cuticle, bark scale, and needle fragment	360 ± 25	319-494	1456-1631 CE
SJC 2.210	*Keck-161818*	*45-50cm*	*Charred cuticle and non-conifer wood (or non-wood)*	*2990 ± 25*	*3077-3228*	*1128-1279 BCE*
SJC 2.217	Keck-163081	80-85cm	Charred cuticle	405 ± 25	335-510	1440-1615 CE
SJC 2.221	*Keck-161819*	*100-105cm*	*Charred cuticle and glassy carbon*	*2700 ± 25*	*2760-2846*	*811-897 BCE*
SJC 2.227	*Keck-163082*	*135-140cm*	*Charred axis and cuticle*	*3070 ± 25*	*3224-3356*	*1275-1407 BCE*
SJC 2.232	Keck-161820	155-160cm	Charred cuticle and needle fragment	1880 ± 25	1737-1878	72-213 CE
SJC 2.136	Keck-168916	180-185cm	charred angiosperm xylem	3845 ± 25	4153-4406	2204-2457 BCE
SJC 2.238	*Keck-161821*	*185-190cm*	*Charred cuticle*	*5570 ± 25*	*6304-6402*	*4355-4453 BCE*

Table S15. **Parameters for modeling scenarios in Fire BGCv2**.

Scenario	Phase	Population size	Fuelwood harvest multiplier (kg/yr)	Simulation years	Fuelwood harvest target (kg/yr)	Ignitions (FRI multiplier)	Agricultural burning (ha/yr)	Live tree Harvest (kg/yr)
LP,LF	Vallecitos	150	1500	201	225,000	0	0	0
LP,LF	Paliza	4000	1500	326	6,000,000	0	0	0
LP,LF	Early Jemez	5000	1500	451	7,500,000	0	0	0
LP,LF	Late Jemez	5000	1500	526	7,500,000	0	0	0
LP,LF	Guadalupe	500	1500	626	750,000	0	0	0
LP,HF	Vallecitos	150	3000	201	450,000	0	0	0
LP,HF	Paliza	4000	3000	326	12,000,000	0	0	0
LP,HF	Early Jemez	5000	3000	451	15,000,000	0	0	0
LP,HF	Late Jemez	5000	3000	526	15,000,000	0	0	0
LP,HF	Guadalupe	500	3000	626	1,500,000	0	0	0
HP,LF	Vallecitos	500	1500	201	750,000	0	0	0
HP,LF	Paliza	7000	1500	326	10,500,000	0	0	0
HP,LF	Early Jemez	8000	1500	451	12,000,000	0	0	0
HP,LF	Late Jemez	8000	1500	526	12,000,000	0	0	0
HP,LF	Guadalupe	3000	1500	626	4,500,000	0	0	0
HP,HF	Vallecitos	500	3000	201	1,500,000	0	0	0
HP,HF	Paliza	7000	3000	326	21,000,000	0	0	0
HP,HF	Early Jemez	8000	3000	451	24,000,000	0	0	0
HP,HF	Late Jemez	8000	3000	526	24,000,000	0	0	0
HP,HF	Guadalupe	3000	3000	626	9,000,000	0	0	0
HP,HF	Vallecitos	500	3000	201	1,500,000	1.5	0	0
HP,HF	Paliza	7000	3000	326	21,000,000	1.5	0	0
HP,HF	Early Jemez	8000	3000	451	24,000,000	1.5	0	0
HP,HF	Late Jemez	8000	3000	526	24,000,000	1.5	0	0
HP,HF	Guadalupe	3000	3000	626	9,000,000	1.5	0	0

LP,SF,MIA	Vallecitos	150	1500	201	225,000	1.225	60	7350
LP,SF,MIA	Paliza	4000	1500	326	6,000,000	7	1600	196000
LP,SF,MIA	Early Jemez	5000	1500	451	7,500,000	8.5	2000	245000
LP,SF,MIA	Late Jemez	5000	1500	526	7,500,000	8.5	2000	245000
LP,SF,MIA	Guadalupe	500	1500	626	750,000	1.75	200	24500
HP,SF,MIA	Vallecitos	500	3000	201	450,000	1.75	200	24500
HP,SF,MIA	Paliza	7000	3000	326	12,000,000	11.5	2800	343000
HP,SF,MIA	Early Jemez	8000	3000	451	15,000,000	13	3200	392000
HP,SF,MIA	Late Jemez	8000	3000	526	15,000,000	13	3200	392000
HP,SF,MIA	Guadalupe	3000	3000	626	1,500,000	5.5	1200	147000
LP,SF,HIA	Vallecitos	150	1500	201	225,000	1.45	240	7350
LP,SF,HIA	Paliza	4000	1500	326	6,000,000	13	6400	196000
LP,SF,HIA	Early Jemez	5000	1500	451	7,500,000	16	8000	245000
LP,SF,HIA	Late Jemez	5000	1500	526	7,500,000	16	8000	245000
LP,SF,HIA	Guadalupe	500	1500	626	750,000	2.5	800	24500
HP,SF,HIA	Vallecitos	500	3000	201	450,000	2.5	800	24500
HP,SF,HIA	Paliza	7000	3000	326	12,000,000	22	11200	343000
HP,SF,HIA	Early Jemez	8000	3000	451	15,000,000	25	12800	392000
HP,SF,HIA	Late Jemez	8000	3000	526	15,000,000	25	12800	392000
HP,SF,HIA	Guadalupe	3000	3000	626	1,500,000	10	4800	147000

SI References

1. P. J. Schoeneberger, D. A. Wysocki, E. C. Benham, Soil Survey Staff, *Field book for describing and sampling soils, Version 3.0.* (Natural Resources Conservation Service, National Soil Survey Center, Lincoln, NE, 2012).

2. P. Bullock, N. Fedoroff, A. Jongerius, G. Stoops, T. Tursina, *Handbook for Soil Thin Section Description* (Waine Research Publications, Mount Pleasant, UK, 1985).

3. G. Stoops, *Guidelines for Analysis and Description of Soil and Regolith Thin Sections* (Soil Science Society of America, Madison, WI, 2003).

4. P. Janitsky, "Particle-size analysis" in Field and Laboratory Procedures Used in a Soil Chronosequence Study, M. Singer, P. Janitsky, Eds. (United States Government Printing Office, Washington, 1986), pp. 11-16.

5. M. G. Winkler, Charcoal analysis for paleoenvironmental interpretation: a chemical assay. *Quaternary Research* **23**, 313-326 (1985).

6. C. Whitlock, R. S. Anderson, "Fire History Reconstructions Based on Sediment Records from Lakes and Wetlands" in Fire and Climatic Change in Temperate Ecosystems of the Western Americas, T. T. Veblen, W. L. Baker, G. Montenegro, T. W. Swetnam, Eds. (Springer, New York, 2003), pp. 3-31.

7. A. N. Rhodes, A Method for the Preparation and Quantification of Microscopic Charcoal from Terrestrial and Lacustrine Sediment Cores. *The Holocene* **8**, 113-117 (1998).

8. F. Brock, T. Higham, P. Ditchfield, C. B. Ramsey, Current Pretreatment Methods for AMS Radiocarbon Dating at the Oxford Radiocarbon Accelerator Unit (Orau). *Radiocarbon* **52**, 103-112 (2010).

9. P. J. Reimer *et al.*, IntCal13 and Marine13 Radiocarbon Age Calibration Curves 0–50,000 Years cal BP. *Radiocarbon* **55**, 1869-1887 (2016).

10. C. E. Buck, J. A. Christen, G. N. James, BCal: on online Bayesian radiocarbon calibration tool. *Internet Archaeology* **7** (1999).

11. M. Blaauw, Methods and code for 'classical' age-modelling of radiocarbon sequences. *Quaternary Geochronology* **5**, 512-518 (2010).

12. G. Dean, Use of pollen concentrations in coprolite analysis: an archaeobotanical viewpoint with a comment to Reinhard et al.(1991). *Journal of Ethnobiology* **13**, 102-114 (1993).

13. P. A. Collinvaux, P. E. De Oliveira, E. Moreno, *Amazon Pollen Manual and Atlas* (Harwood Academic Publishers, Amsterdam, 1999).

14. V. M. Bryant, S. A. Hall, Archaeological Palynology in the United States: A Critique. *American Antiquity* **58**, 277-286 (1993).

15. A. Traverse, *Paleopalynology* (Springer Science & Business Media, New York, 2007), vol. 28.

16. R. O. Kapp, *How to know pollen and spores* (William C. Brown Company Publishers, Dubuque, 1969).

17. P. D. Moore, M. E. Collinson, J. A. Webb, *Pollen Analysis* (Blackwell Publishers, Oxford, ed. Second edition, 1991).

18. R. Buchner, M. Weber (2000) PalDat-a palynological database: Descriptions, illustrations, identification and information retrieval. in *Society for the Promotion of Palynological Research in Austria (paldat.org)*.

19. R Core Team, *R: A Language and Environment for Statistical Computing* (R Foundation for Statistical Computing, Vienna, Austria, 2020).

20. J. W. Williams *et al.*, The Neotoma Paleoecology Database, a multiproxy, international, community-curated data resource. *Quaternary Research* **89**, 156-177 (2018).

21. D. Battistel *et al.*, GC-MS method for determining faecal sterols as biomarkers of human and pastoral animal presence in freshwater sediments. *Analytical and Bioanalytical Chemistry* **407**, 8505-8514 (2015).

22. J. H. Fink, C. R. Manley, "Explosive Volcanic Activity Generated from Within Advancing Silicic Lava Flows" in Volcanic Hazards*,* J. H. Latter, Ed. (Springer, Berlin, 1989), pp. 169-179.

23. J. D. Pelletier *et al.*, Calibration and testing of upland hillslope evolution models in a dated landscape: Banco Bonito, New Mexico. *Journal of Geophysical Research: Earth Surface* **116**, F04004 (2011).

24. S. Kelley *et al.* (2003) Geologic Map of the Jemez Springs Quadrangle, Sandoval County, New Mexico. in *Open-file Digital Geologic Map OF-GM 073* (New Mexico Bureau of Geology and Mineral Resources, Socorro).

25. W. Phillips, J. Poths, F. Goff, S. Reneau, E. McDonald (1997) Ne-21 surface exposure ages from the Banco Bonito obsidian flow, Valles caldera, New Mexico, USA. in *Geological Society of America, Abstracts with Programs*, pp A-419.

26. K. Lepper, F. Goff, Yet another attempt to date the Banco Bonito rhyolite, the youngest volcanic flow in the Valles caldera, New Mexico. *New Mexico Geology* **29**, 117-121 (2007).

27. T. W. Swetnam, C. H. Baisan, "Tree-ring reconstructions of fire and climate history of the Sierra Nevada and Southwestern United States" in Fire and Climate Change in Temperate Ecosystems of the Western Americas*,* T. T. Veblen, C. M. Baker, G. Montenegro, T. W. Swetnam, Eds. (Springer, New York, NY, 2003), pp. 158-195.

28. C. D. Allen, R. S. Anderson, R. B. Jass, J. L. Toney, C. H. Baisan, Paired charcoal and tree-ring records of high-frequency Holocene fire from two New Mexico bog sites. *International Journal of Wildland Fire* **17**, 115-130 (2008).

29. W. Catchpole, "Fire properties and burn patterns in heterogeneous landscapes" in Flammable australia: The fire regimes and biodiversity of a continent*,* R. A. Bradstock, J. E. Williams, A. M. Gill, Eds. (Cambridge University Press, Cambridge, UK, 2002), pp. 49-75.

30. M. G. Rollins, LANDFIRE: a nationally consistent vegetation, wildland fire, and fuel assessment. *International Journal of Wildland Fire* **18**, 235-249 (2009).

31. J. A. Clark, R. A. Loehman, R. E. Keane, Climate changes and wildfire alter vegetation of Yellowstone National Park, but forest cover persists. *Ecosphere* **8**, e01636 (2017).

32. R. A. Loehman, J. A. Clark, R. E. Keane, Modeling effects of climate change and fire management on western white pine (Pinus monticola) in the northern Rocky Mountains, USA. *Forests* **2**, 832-860 (2011).

33. P. E. Thornton, S. W. Running, An improved algorithm for estimating incident daily solar radiation from measurements of temperature, humidity, and precipitation. *Agricultural and Forest Meteorology* **93**, 211-228 (1999).

34. P. M. Brown, M. W. Kaye, L. S. Huckaby, C. H. Baisan, Fire history along environmental gradients in the Sacramento Mountains, New Mexico: Influences of local patterns and regional processes. *Ecoscience* **8**, 115-126 (2001).

35. W. W. Covington *et al.*, Restoring ecosystem health in ponderosa pine forests of the Southwest. *Journal of Forestry* **95**, 23-29 (1997).

36. E. Q. Margolis, C. A. Woodhouse, T. W. Swetnam, Drought, multi-seasonal climate, and wildfire in northern New Mexico. *Climatic Change* **142**, 433-446 (2017).

37. D. W. Huffman, P. Z. Fulé, K. M. Pearson, J. E. Crouse, Fire history of pinyon–juniper woodlands at upper ecotones with ponderosa pine forests in Arizona and New Mexico. *Canadian Journal of Forest Research* **38**, 2097–2108 (2008).

38. R. Touchan, C. D. Allen, T. W. Swetnam, "Fire History and Climatic Patterns in Ponderosa Pine and Mixed-Conifer Forests of the Jemez Mountains, Northern New Mexico" in Fire Effects in Southwestern Forests: Proceedings of the Second La Mesa Fire Symposium, Los Alamos, New Mexico, March 29-31, 1994*,* C. D. Allen, Ed. (U.S. Department of Agriculture, Forest Service, Rocky Mountain Research Station, Fort Collins, CO., 1996), pp. 33-46.

39. T. W. Swetnam, C. H. Baisan, "Historical Fire Regime Patterns in the Southwestern United States Since AD 1700" in Fire Effects in Southwestern Forests: Proceedings of the Second La Mesa Fire Symposium, Los Alamos, New Mexico, March 29-31, 1994*,* C. D. Allen, Ed. (U.S. Department of Agriculture, Forest Service, Rocky Mountain Research Station, Fort Collins, CO., 1996), pp. 11-32.

40. G. Gottfried, T. Swetname, C. Allen, J. Betancourt, A. Chung-MacCoubrey, "Pinyon-juniper woodlands. Ecology, diversity and sustainability of the middle Rio Grande Basin" in Ecology, Diversity, and Sustainability of the Middle Rio Grande Basin*,* D. M. Finch, J. A. Tainter, Eds. (USDA Forest Service - Rocky Mountain Research Station, Fort Collins, CO, 1995), vol. Volume RM-GTR-268, pp. 95-132.

41. FEIS (2015) Fire Effects Information System [online]. (U.S. Department of Agriculture, Forest Service, Rocky Mountain Research Station, Fire Sciences Laboratory, Missoula, MT).

42. P. Z. Fulé, W. W. Covington, M. M. Moore, Determining Reference Conditions for Ecosystem Management of Southwestern Ponderosa Pine Forests. *Ecological Applications* **7**, 895-908 (1997).

43. D. C. Chojnacky, *Volume equations for New Mexico's pinyon-juniper dryland forests* (U. S. Department of Agriculture, Forest Service, Intermountain Research Experiment Station, 1994), vol. Research Paper INT-471.